

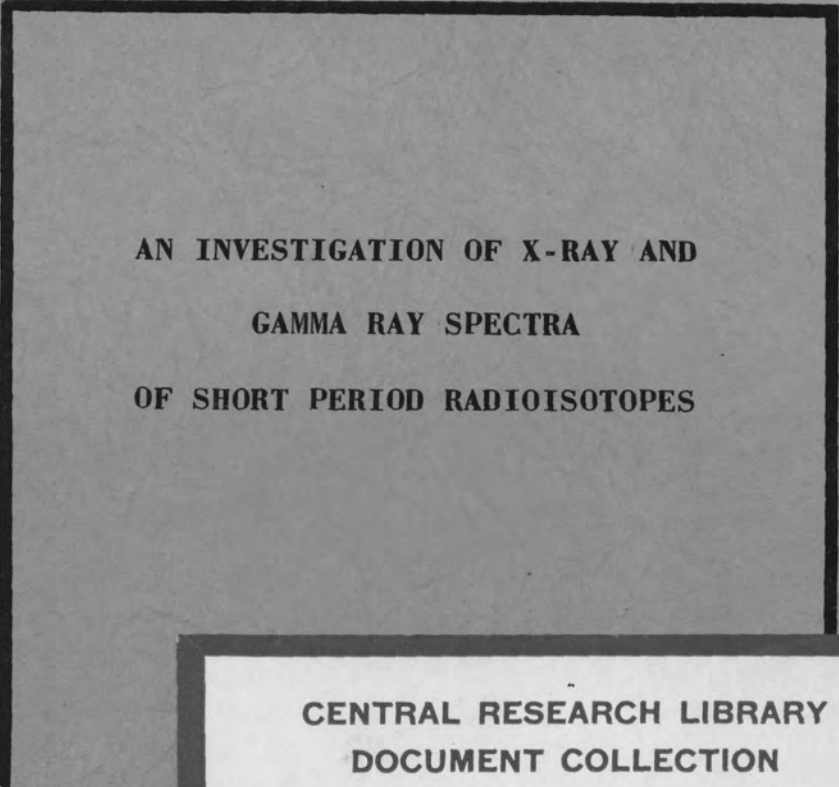
UNCLASSIFIED

MARTIN MARIETTA ENERGY SYSTEMS LIBRARIES

3 4456 0360888 9

ORNL 1089
Physics
8a

CENTRAL RESEARCH LIBRARY
DOCUMENT COLLECTION



AN INVESTIGATION OF X-RAY AND
GAMMA RAY SPECTRA
OF SHORT PERIOD RADIOISOTOPES



CENTRAL RESEARCH LIBRARY
DOCUMENT COLLECTION
LIBRARY LOAN COPY
DO NOT TRANSFER TO ANOTHER PERSON
If you wish someone else to see this document,
send in name with document and the library will
arrange a loan.

OAK RIDGE NATIONAL LABORATORY
OPERATED BY
CARBIDE AND CARBON CHEMICALS COMPANY
A DIVISION OF UNION CARBIDE AND CARBON CORPORATION



POST OFFICE BOX P
OAK RIDGE, TENNESSEE

UNCLASSIFIED

UNCLASSIFIED

ORNL- 1089

Physics
This document consists of
90 pages.
Copy 8 of 241 Series A.

Contract No. W-7405, eng. 26

Physics Division

AN INVESTIGATION OF X-RAY AND GAMMA RAY SPECTRA
OF SHORT PERIOD RADIOISOTOPES*

by

Jack H. Kahn**

Date Issued:

001 1953

OAK RIDGE NATIONAL LABORATORY
operated by
CARBIDE AND CARBON CHEMICALS DIVISION
Union Carbide and Carbon Corporation
Post Office Box P
Oak Ridge, Tennessee

* Submitted in partial fulfillment of the requirements for the degree of Doctor of Philosophy at the University of Tennessee.

** This work was performed while the author was a Graduate Fellow of the Oak Ridge Institute of Nuclear Studies at the Oak Ridge National Laboratory operated for the U. S. Atomic Energy Commission by Carbide and Carbon Chemicals Division

UNCLASSIFIED



3 4456 0360888 9

ORNL 1089
Physics

INTERNAL DISTRIBUTION

1. G. T. Felbeck (C&CCC)	23. R. C. Briant	40. L. D. Roberts
2-3. Chemistry Library	24. J. A. Swartout	41. R. N. Lyon
4. Physics Library	25. S. C. Lind	42. W. C. Koehler
5. Biology Library	26. F. L. Steahly	43. W. K. Ergen
6. Health Physics Library	27. A. Hollaender	44. E. P. Blizard
7. Metallurgy Library	28. M. T. Kelley	45. M. E. Rose
8-9. Training School Library	29. G. H. Clewett	46. M. J. Skinner
10-13. Central Files	30. K. Z. Morgan	47-48. E. C. Campbell
14. C. E. Center	31. J. S. Felton	49. J. W. T. Dabbs, Jr.
15. C. E. Larson	32. A. S. Householder	50-59. J. H. Kahn - Box 187, Boliver, Tenn.
16. W. B. Humes (K-25)	33. C. S. Harrill	60. F. K. McGowan
17. W. D. Lavers (Y-12)	34. C. E. Winters	61. Kathleen L. Robertson
18. A. M. Weinberg	35. D. S. Billington	62. C. P. Stanford
19. E. H. Taylor	36. D. W. Cardwell	63. T. E. Stephenson
20. E. D. Shipley	37. E. M. King	64. C. J. Borkowski
21. A. H. Snell	38. E. O. Wollan	65-66. Central Files (O.P.)
22. F. C. VonderLage	39. C. B. Ellis	

EXTERNAL DISTRIBUTION

67-78. Argonne National Laboratory
79. Armed Forces Special Weapons Project
80-85. Atomic Energy Commission, Washington
86. Battelle Memorial Institute
87. Brush Beryllium Company
88-91. Brookhaven National Laboratory
92. Brookhaven National Laboratory (Attn: M. Goldhaber)
93. Brookhaven National Laboratory (Attn: E. der Mateosian)
94. Brookhaven National Laboratory (Attn: S. A. Goudsmit)
95. Brookhaven National Laboratory (Attn: A. W. Sunyar)
96. Brookhaven National Laboratory (Attn: W. Bernstein)
97. Bureau of Medicine and Surgery
98. Bureau of Ships
99-102. Carbide and Carbon Chemicals Company (K-25 Plant)
103. Columbia University (J. R. Dunning)
104. Columbia University (G. Failla)
105-109. E. I. du Pont de Nemours and Company
110-113. General Electric, Richland
114-117. Idaho Operations Office
118-119. Iowa State College
120. Kansas City Operations Branch
121. Kellex Corporation
122-123. Kirtland Air Force Base
124-127. Knolls Atomic Power Laboratory
128-130. Los Alamos Scientific Laboratory

- 131. Louisiana State University (Attn: M. Goodrich)
- 132. Mallinckrodt Chemical Works
- 133. Massachusetts Institute of Technology (A. Gaudin)
- 134. Massachusetts Institute of Technology (A. R. Kaufmann)
- 135-137. Mound Laboratory
- 138. National Advisory Committee for Aeronautics
- 139. National Bureau of Standards (R. D. Huntoon)
- 140. Naval Medical Research Institute
- 141-142. Naval Radiological Defense Laboratory
- 143. New Brunswick Laboratory
- 144-146. New York Operations Office
- 147. North American Aviation, Inc.
- 148-151. Carbide and Carbon Chemicals Company (Y-12 Area)
- 152. Patent Branch, Washington
- 153. Purdue University (Attn: E. Bleuler)
- 154. Purdue University (Attn: R. M. Steffen)
- 155. RAND Corporation
- 156. Sandia Corporation
- 157. Santa Fe Operations Office
- 158. Savannah River Operations Office (Wilmington)
- 159. Stanford University (Attn: R. Hofstadter)
- 160-174. Technical Information Service, Oak Ridge
- 175-176. U. S. Geological Survey (T. B. Nolan)
- 177-178. U. S. Public Health Service
- 179. University of California at Los Angeles
- 180-184. University of California Radiation Laboratory
- 185. University of Illinois (Attn: F. R. Metzger)
- 186-187. University of Rochester
- 188. University of Tennessee (Library)
- 189. University of Tennessee (Attn: Prof. R. D. Present)
- 190. University of Tennessee (Attn: Prof. A. H. Nielsen)
- 191. University of Washington
- 192. Western Reserve University
- 193-196. Westinghouse Electric Corporation
- 197. Yale University
- 198-201. Atomic Energy Project, Chalk River
- 202. Chief of Naval Research
- 203. H. K. Ferguson Company
- 204. Harshaw Chemical Company
- 205. Isotopes Division (Mr. McCormick)
- 206-207. Library of Congress, Acquisition Department (J. W. Cormn)
- 208. National Bureau of Standards
- 209. National Research Council, Ottawa
- 210. Naval Research Laboratory
- 211-212. Nevis Cyclotron Laboratories
- 213-214. Oak Ridge Institute of Nuclear Studies
- 215-224. United Kingdom Scientific Mission (M. Greenhill)
- 225. USAF, Eglin Air Force Base (Technical Library)
- 226. USAF, Wright-Patterson Air Force Base (Rodney Nudenberg)
- 227-231. USAF, Wright-Patterson Air Force Base (CADO)

- 232. U. S. Army, Army Field Forces (Captain James Kerr)
- 233. U. S. Army, Atomic Energy Branch (Lt. Col. A. W. Betts)
- 234. U. S. Army, Director of Operations Research (Dr. Ellis Johnson)
- 235. U. S. Army, Office, Chief of Ordnance (Col. A. R. Del Campo)
- 236-237. U. S. Army, Office of the Chief Signal Officer (Curtis T. Clayton
thru Major George C. Hunt)
- 238-240. U. S. Army, Technical Command (Col. J. H. Rothschild
Attn: Technical Library)
- 241. UT-AEC Agricultural Research Program (Charles S. Hobbs)

ACKNOWLEDGMENTS

It is a pleasure for the author to acknowledge his appreciation to Dr. E. C. Campbell for his aid and advice in the planning and development of this research. The author is also indebted to Mr. P. R. Bell, Prof. A. H. Nielsen, and Prof. R. D. Present for numerous stimulating discussions concerning the results; to Mrs. K. L. Robertson for making the photographic prints; and to the entire Physics Division of the Oak Ridge National Laboratory without whose cooperation this dissertation could not have been completed.

The author gratefully acknowledges the grant of a Fellowship from the Oak Ridge Institute of Nuclear Studies to pursue this research.

TABLE OF CONTENTS

CHAPTER	PAGE
I. INTRODUCTION	1
Statement of the Present Research	1
Theory of Nuclear Isomerism	2
Internal Conversion	11
Detection of Gamma Rays	13
II. APPARATUS.	18
Proportional Counters	18
Sodium Iodide Crystal Detectors	22
Electronic Equipment.	23
Preparation of Samples.	25
III. EXPERIMENTAL RESULTS	27
Preliminary Tests	27
Calibration of the Proportional Counter Spectrometer.	34
Counter Efficiency.	43
Accuracy of Energy Measurements	47
Gamma and X-ray Spectra of Various Short Period Activities	48
IV. ANALYSIS OF DATA	70
Partial Internal Conversion Coefficients.	70
Conclusion.	73
Summary	78
BIBLIOGRAPHY	79

LIST OF TABLES

TABLE	PAGE
I. Selection Rules for Multipole Radiation	8
II. Approximate Expected Half-lives for Gamma Emission for Element with $A = 100$	10
III. Partial Internal Conversion Coefficients.	71
IV. Summary of Experimental Data.	75

LIST OF FIGURES

FIGURE	PAGE
1. Block Diagram of Spectrometer	24
2. K X-rays from Sb^{122}	28
3. K X-rays from Cd^{109}	28
4. Fluorescent X-rays from Thin Metal Foils.	33
5. X-rays from Cd^{109} as Detected by Krypton Counter.	35
6. X-rays from Cd^{109} as Detected by Xenon Counter.	39
7. X-ray from Eu^{152} as Detected by Xenon Counter	41
8. Absorption Curve for Xenon Counter.	44
9. Efficiency of Xenon Counter as a Function of γ and X-ray Energy.	46
10. Spectrum of Co^{60} (10.7 min)	49
11. Spectrum of Se^{77} (17.5 sec)	49
12. Spectrum of Zr (5 sec).	51
13. K X-rays from Zr, Cb, and Mo Detected with Krypton Counter	53
14. Spectrum of Rh^{104} (4.7 min)	55
15. K X-rays from Rhodium Detected with Krypton Counter	55
16. Spectrum of Pd (5 min).	56
17. Spectrum of In (2.5 sec).	56
18. Spectrum of Sb^{122} (3.5 min)	58
19. Spectrum of Dy^{165} (1.25 min).	58
20. Spectrum of Yb (< 0.5 and 6 sec).	61
21. Spectrum of Hf^{179} (19 sec).	61

FIGURE	PAGE
22. Spectrum of Ta (0.33 sec)	64
23. Spectrum of W (5.5 sec)	64
24. Spectrum of Ir ¹⁹² (1.5 min)	66
25. Spectrum of U ²³⁹ (23.5 min)	66
26. Gamma and X-radiation from Various Radioactive Nuclei	69
27. Half-life Energy Relations for $ \Delta \vec{I} = 3$ Transitions.	77

CHAPTER I

INTRODUCTION

Statement of the Present Research

As a preliminary step in the present research, a search for new short period nuclear isomers was made using the scintillation spectrometer constructed by Campbell and Goodrich.¹ Neutron induced gamma rays with half-lives of the order of a second have been detected and their energies measured. An unreported activity has been found in each of the three following elements: palladium, indium, and ytterbium.

In order to observe x-rays and low energy gamma rays (less than 75 kev) a proportional counter was added to the apparatus. For low energy radiation a proportional counter is more accurate than a scintillation counter, but the upper energy limit for measuring gamma radiation with a proportional counter is smaller by a factor of nearly 100 compared to that obtainable with a scintillation counter.

Fifteen short period neutron induced gamma activities believed to be nuclear isomers are discussed herein. Although decay schemes were not investigated in most cases, it was discovered that in the case of the 3.5 minute antimony isomer a double transition exists rather than a single gamma ray as previously reported.

Partial internal conversion coefficients have been calculated in

¹E. C. Campbell and M. Goodrich, Phys. Rev. 78, 640 (1950).

four cases by comparing the number of characteristic x-rays with the number of gamma rays emitted by the radioactive isotope. This method of determining the internal conversion coefficient is only applicable in cases where the decay scheme is known.

X-rays from three radioactive elements have been positively identified either by the critical absorption method or by comparison with known fluorescent x-rays. The fluorescent yield for krypton and xenon has been measured.

Theory of Nuclear Isomerism

According to present ideas of nuclear structure, the nucleus is constituted of protons and neutrons. A system of Z protons and N neutrons will, if it is stable at all, be able to exist in one or more stationary states. If the system is in an excited state, there is a certain probability for the transition to the ground state by the emission of one or more gamma rays. The half-life of an excited level is as a rule less than 10^{-12} sec. Sometimes it occurs, however, that the half-life is of much greater length. In such a case a metastable state is said to exist, and the metastable state and the ground state are called isomeric nuclei. The limit between metastable states and ordinary excited states is not a well-defined one; however, for practical purposes it is convenient to speak of isomers only in the case in which the half-life is long enough to allow a direct observation. Thus the half-lives of metastable states may range from 10^{-10} sec to several months.

Nuclear isomerism was not much studied until the discovery of artificial radioactivity. The first investigations of neutron induced

radioactivity by Fermi and others² resulted in the observation of several activities which have later turned out to be cases of nuclear isomerism. Some of these will be discussed in detail later.

One of the first theoretical discussions on nuclear isomerism was given by von Weizsäcker.³ He pointed out that nuclear isomerism might be explained by the assumption that there is a large difference of spin between the metastable state and the ground state.

Von Weizsäcker gave the formula

$$P(L) \leq \frac{Z^2 e^2 E}{\hbar^2 c} \left(\frac{ER}{\hbar c} \right)^{2L}. \quad (1)$$

where $P(L)$ means the probability per unit time of a transition between two nuclear states by the emission of gamma radiation of electric multipole order 2^L . E is the energy difference between the two states and L the magnitude of the vector spin difference. The other symbols have their usual meanings. This formula gives, when reasonable values of energy and spin difference are inserted, half-lives of sufficient length to make nuclear isomerism possible.

The transition between two energy states of a nucleus does not necessarily consist in the emission of a gamma ray. As the outer electrons, especially those of the K and L shells, constitute a perturbation of the nucleus, energy may be transferred directly from the nucleus to an

²E. Fermi, E. Amaldi, O. D'Agostino, F. Rasetti, and E. Segrè, Proc. Roy. Soc. A146, 483 (1934); and E. Amaldi, O. D'Agostino, E. Fermi, B. Pontecorvo, F. Rasetti and E. Segrè, Proc. Roy. Soc. A149, 522 (1935).

³C. F. von Weizsäcker, Naturwiss. 24, 813 (1936).

outer electron which is liberated from the atom. This process is known as internal conversion. When this phenomenon was observed in the disintegration of radium, it was first considered as a consequence of the primary beta rays that were emitted.

The relation between these energetically homogeneous electron groups (conversion electrons) and the accompanying gamma rays was pointed out by Ellis.⁴ He suggested that the energies of the homogeneous groups of electrons emitted by natural radioactive elements are equal to the energy characteristic only of a particular gamma ray minus the energy necessary to remove the electron from the atom. This he verified by measuring the energy of the line spectra produced when various elements were irradiated by given gamma rays. To the measured energy of each homogeneous electron group was added the K absorption energy (which had been obtained from x-ray data) of the element from which it came, and within the limits of experimental error the same energy for a given gamma ray was obtained from each element.

In many nuclear reactions and radioactive transformations the product nucleus is left in an excited state. In making an isomeric transition (that is, a transition of a metastable state to a lower energy state of the same nucleus), a nucleus may give energy either to a gamma ray or to an extra-nuclear electron by the internal conversion process. The title "internal conversion" suggesting as it does that a gamma ray is first emitted and then absorbed by an extra-nuclear electron, is rather misleading, in view of the modern theory according to which the emission

⁴C. D. Ellis, Proc. Roy. Soc. A99, 261 (1921).

of a conversion electron is due to a direct interaction between the nucleus and the electron ejected. Experimentally, it is not possible to distinguish the two step process in which (1) a photon is emitted, and (2) this photon is absorbed by a bound electron, from the case in which the electron perturbs the nucleus and induces a transition to a lower energy state with the transition energy being transferred to the electron.

Regardless of how one views the mechanical details of the conversion process, the transition energy is equal to the energy of the gamma ray, which in turn is equal to the energy of the conversion electron plus the binding energy of this electron in its atomic level. As a result there may be several conversion electrons characteristic of any single gamma ray depending in which level the conversion electron originates.

The internal conversion of a gamma ray leaves the atom ionized in an inner electron shell. When this shell fills, the atom emits characteristic x-ray lines. Sometimes, however, instead of the emission of an x-ray quantum an Auger electron may be ejected. This will be discussed in more detail later. The identification of the characteristic x-rays emitted following internal conversion makes it possible to assign the gamma ray transition to a definite element.

The ratio between the number of K electrons ejected by internal conversion and the number of gamma quanta emitted is called the partial internal conversion coefficient for the K shell,* or symbolically

$$\alpha_K = \frac{N_K}{N_\gamma} \quad (2)$$

Similar definitions hold for the other shells. The ratio between the

*This exceeds the older definition by a factor $1 + \alpha$.

total number of electrons ejected and the number of gamma quanta emitted is simply called the internal conversion coefficient. The internal conversion coefficient is thus the sum of the partial conversion coefficients, or symbolically

$$\alpha = \alpha_K + \alpha_{L_I} + \alpha_{L_{II}} + \alpha_{L_{III}} + \alpha_M + \dots = \frac{N_e}{N_\gamma} \quad (3)$$

in which N_e is the total number of conversion electrons emitted.

The mean life for gamma emission depends chiefly upon (1) the difference in energy between the two levels, (2) the value of the nuclear angular momentum in the initial and final states, and (3) the parity change. Conservation of relativistic total energy and of total angular momentum applies to the system nucleus plus the photon. It is clear that (1) above determines the photon energy, and (2) gives the possible values of angular momentum which are carried away by the photon (i.e.

$|I' - I| \dots I' + I$ where I' and I are the angular momentum of the initial and final states in \hbar units). The angular momentum of the photon is equal to the vector change in the nuclear angular momentum.

The vector spin change $\Delta \vec{I}$ for a gamma transition cannot be zero because the intrinsic spin of a photon is at least one. For $|\Delta \vec{I}| = 1$, the mean life is practically always $< 10^{-12}$ seconds; within the resolving time of present-day detectors, gamma emission takes place "immediately" after the nucleus is formed in its excited state.

Gamma emission processes are classified according to their multipole order. These classifications are assigned according to the vector

change in the nuclear angular momentum, and to the change in parity that the nucleus experiences during the transition. For example if a nucleus has an excited state with angular momentum I' and a fundamental state with angular momentum I , the radiation of the lowest order, that is, the most probable one will be an electric or magnetic multipole of order 2^L where $L = |I' - I|$. If $L = 1$, the multipole order is 2, and the transition is called dipole. The parity change for the nucleus determines the nature of the multipole transition. The parity of a quantum state is odd (-) or even (+) according to whether a reversal of the sign of all coordinates exclusive of spin does or does not reverse the sign of the wave function describing the state. If a nucleus has an excited and fundamental state that are both odd or both even, then the transition between them involves only electric multipoles of even order and magnetic multipoles of odd order. If the two states are of opposite parity (one being even and one odd) electric multipoles of odd order and magnetic multipoles of even order can alone contribute to the transition. The lowest allowed multipoles of the two types are summarized in Table I.

Weisskopf⁵ calculated the following expressions for the multipole radiation probabilities for electric and magnetic radiation of order L respectively.

$$P_E(L) = \frac{4.4(L+1)}{L[1 \cdot 3 \cdot 5 \cdot (2L+1)]^2} \left[\frac{E}{197} \right]^{2L+1} R^{2L} \times 10^{21} \text{ sec}^{-1} \quad (4)$$

$$P_M(L) = \frac{0.19(L+1)}{L[1 \cdot 3 \cdot 5 \cdot (2L+1)]^2} \left[\frac{E}{197} \right]^{2L+1} R^{2(L-1)} \times 10^{21} \text{ sec}^{-1} \quad (5)$$

⁵Privately circulated notes to appear as part of a book on nuclear physics.

UNCLASSIFIED
 DWG. 11776

TABLE I
 SELECTION RULES FOR MULTIPOLE RADIATION

	L EVEN	L ODD
PARITY OF STATES EQUAL (+, + OR -, -)	ELECTRIC 2^L POLE	ELECTRIC 2^{L+1} POLE
	MAGNETIC 2^{L+1} POLE	MAGNETIC 2^L POLE
PARITY OF STATES OPPOSITE (+, - OR -, +)	ELECTRIC 2^{L+1} POLE	ELECTRIC 2^L POLE
	MAGNETIC 2^L POLE	MAGNETIC 2^{L+1} POLE

in which E is the transition energy in Mev, and R is the nuclear radius in units of 10^{-13} cm. Because of the lack of knowledge about the interior of the nucleus this formula is claimed to be valid only to within a factor $\sim 10^{\pm 2}$.

Table II shows the estimated half-lives given by these formulas for various fictitious gamma radiations from a nucleus having $R = 1.5 \times (100)^{1/3} \times 10^{-13}$ cm. (i.e. $A = 100$). These results apply only to a bare nucleus, and do not include the extra transitions induced by the perturbations of the orbital electron cloud.

Neither L nor the parity change is directly observable from gamma radiation. As a result, a direct examination of the gamma rays from a radioactive sample will not disclose the nature of the transition that gave rise to them. However, a knowledge of the half-life and energy, the internal conversion coefficient, and angular correlation between successive gamma rays gives information regarding the order and the type of the radiation.

If conversion electrons are emitted when a nucleus goes from an excited state to a lower state, the observed lifetime will be less than the estimated lifetime for gamma emission. According to Taylor and Mott⁶ the actual decay constant is given to a very good approximation by the sum of the decay constant for the gamma radiation with a bare nucleus and the decay constant corresponding to the transition probability induced by the electrons. Thus the half-life of an excited state, τ , is given by

⁶H. M. Taylor and N. F. Mott, Proc. Roy. Soc. A142, 215 (1933).

UNCLASSIFIED
 DWG. 11912

TABLE II
 APPROXIMATE EXPECTED HALF-LIVES FOR
 GAMMA EMISSION FOR ELEMENT WITH A=100

E_γ (MEV)	TYPE	L=1	L=2	L=3	L=4	L=5
0.01	ELEC.	10^{-10} SEC.	$10^{-1.5}$ SEC.	10^7 SEC.	10^{16} SEC.	10^{25} SEC.
	MAG.	10^{-7} SEC.	$10^{1.5}$ SEC.	10^{10} SEC.	10^{19} SEC.	10^{28} SEC.
0.10	ELEC.	10^{-13} SEC.	$10^{-6.5}$ SEC.	1 SEC.	10^7 SEC.	10^{14} SEC.
	MAG.	10^{-10} SEC.	$10^{-3.5}$ SEC.	10^3 SEC.	10^{10} SEC.	10^{17} SEC.
1.0	ELEC.	10^{-16} SEC.	$10^{-11.5}$ SEC.	10^{-7} SEC.	10^{-2} SEC.	10^3 SEC.
	MAG.	10^{-13} SEC.	$10^{-8.5}$ SEC.	10^{-4} SEC.	10 SEC.	10^6 SEC.

$$\gamma = \frac{0.69}{P_{E,M} + P_e} = \frac{0.69}{P_{E,M} (1 + \alpha)} \quad (6)$$

in which $P_{E,M}$ may be obtained from equation (4) or (5), and α is the internal conversion coefficient.

Internal Conversion

The mechanism by which a K or L electron is emitted in a nuclear transition has been described by Taylor and Mott.⁷ The nucleus consists of a quantum-mechanical system carrying a charge, which possesses a series of stationary states, and it is in an excited state when gamma rays are about to be emitted. An electron in the external atomic system can thus interact with the electromagnetic field of the nucleus. As a first approximation in which the retardation is neglected, the energy of interaction of the electron and the nucleus is given by

$$\Phi = \iint \frac{\rho_N \rho_e}{|\vec{\gamma}_N - \vec{\gamma}_e|} dV_N dV_e \quad (7)$$

in which $\vec{\gamma}_N$ and $\vec{\gamma}_e$ are respectively the position vectors of a nuclear particle and the electron from the center of gravity of the nucleus, and ρ_N and ρ_e are the corresponding charge densities. If $|\vec{\gamma}_e| > |\vec{\gamma}_N|$, which will always be true if the contribution from the region inside the nucleus is neglected, one may make the Taylor expansion

⁷H. M. Taylor and N. F. Mott, Proc. Roy. Soc. A138, 665 (1932).

$$\begin{aligned} \Phi &\approx \iint \frac{\rho_N \rho_e dV_N dV_e}{(\gamma_e^2 - 2\vec{\gamma}_e \cdot \vec{\gamma}_N)^{1/2}} = \iint \frac{\rho_N \rho_e dV_N dV_e}{\gamma_e \left(1 - \frac{2\vec{\gamma}_e \cdot \vec{\gamma}_N}{\gamma_e^2}\right)^{1/2}} \\ &= \iint \rho_N \rho_e dV_N dV_e \left[\frac{1}{\gamma_e} + \frac{\vec{\gamma}_e \cdot \vec{\gamma}_N}{\gamma_e^3} + \text{terms of higher order} \right] \end{aligned} \quad (8)$$

Since $\rho_N = \psi_{iN}^* \psi_{fN}$ with ψ_{iN} and ψ_{fN} orthogonal, it is clear that the first term gives no transitions and that the second term is of the form

$$\Phi_2 = \vec{D}_N \cdot \int dV_e \psi_{fe}^* \psi_{ie} \frac{\vec{\gamma}_e}{\gamma_e^3} \sim \frac{|\vec{D}_N|}{\langle \gamma_e^2 \rangle_{\text{ave}}} \quad (9)$$

where $\vec{D}_N = \int \rho_N \vec{\gamma}_N dV_N$ is the dipole moment of the nuclear charge distribution. The quantity $\frac{\vec{D}_N \cdot \vec{\gamma}_e}{\gamma_e^3}$ is just the static potential for a dipole of moment \vec{D}_N situated at the origin.

In the same way it can be shown that the third term will be of the order $\frac{Q_N}{\langle \gamma^3 \rangle_{\text{ave}}}$ in which $Q_N = \iint \rho_N \gamma_N^2 dV_N$ is related to the quadrupole moment of the nuclear charge distribution. In general the succeeding terms will depend on the various nuclear 2^L pole moments, and the transition probability of the electrons from state ψ_{ie} to state ψ_{fe} will vary roughly as $|\Phi|^2$.

The internal conversion coefficients can be accurately calculated

for any specified multipole order for either electric or magnetic radiation. The calculations are in general exceedingly complicated and are beyond the scope of this dissertation. Rose and his co-workers⁹ have made extensive calculations of the K conversion coefficients for electric and magnetic multipole radiation in the relativistic case with the unscreened coulomb field acting on the electron. Gellman, Griffith and Stanley¹⁰ have made similar calculations for the L_I shell for electric dipole, electric quadrupole and magnetic dipole radiation

Detection of Gamma Rays

Gamma rays originate in the excited nuclei of atoms and they represent the energy difference between an excited state and a lower energy state which may or may not be the ground level of the nucleus. That is, between the initial and the ground states there may exist several possible energy levels. A brief survey of the several ways in which the energy of a gamma ray may be experimentally measured follows.

⁹M. E. Rose, G. H. Goertzel, B. I. Spinrad, J. Harr and P. Strong, Phys. Rev. 83, 79 (1951).

¹⁰H. Gellman, B. A. Griffith and J. P. Stanley, Phys. Rev. 80, 866 (1950).

Crystal Reflection Method

Since gamma radiation consists of electromagnetic waves, physically identical in nature to very penetrating x-rays, the wave length of gamma radiation can be determined by the same technique used in evaluating the wave lengths of x-rays. It was shown by Bragg that x-rays of wave length λ incident on a crystal at a grazing angle θ would be reflected if the equation

$$n \lambda = 2d \sin\theta \quad (n = 1, 2, 3 \dots)$$

were satisfied, where d is the lattice distance of the crystal. An intensely radioactive source is required since the crystal subtends only a small solid angle at the source and since the intensity of the reflected beam is only a small fraction of the intensity of the incident beam. Crystal reflection measurements of gamma ray energies yield greater accuracy than any other method. The range of applicability of the instrument is limited by two difficulties. For energetic gamma radiation the wave length λ becomes so small that no satisfactory crystal lattice is known capable of satisfying the Bragg law with a reflecting angle θ large enough to be accurately determined; and furthermore, the reflecting power of the crystal planes diminishes with diminishing wave length λ about as λ^2 , thus causing a rapid loss in intensity at high energies. Lind, Brown and DuMond¹¹ have recently measured gamma rays with energies above 1 Mev by this method.

Absorption Method

Gamma ray energies are frequently measured by their absorption in

¹¹D. A. Lind, J. R. Brown and J. W. DuMond, Phys. Rev. 76, 1838 (1949).

various materials such as lead, tin, copper, aluminum, etc. This method is reliable if only one or two gamma rays are present and if the two gamma rays are of energies not too close to each other. The energy of the gamma ray is obtained by comparing its absorption with that of gamma rays of known energy in the same absorbing material. In practice, standard curves¹² are used relating energy to the thickness of absorber required to reduce the intensity of the radiation incident on the absorber by a given amount. This method has an accuracy ~ 10 per cent.

Secondary Electron Method

Another procedure for determining the energy of a gamma ray is by measurement of the energy of secondary electrons produced by the interaction of the gamma ray with matter. These electrons may be either Compton recoil electrons, photoelectrons, or pair production electrons.

Photoelectrons are ejected mainly from the K shell provided that the energy of the incident gamma ray is sufficient to ionize the K level of the target atom. This produces a homogeneous group of electrons with energy equal to that of the incident gamma ray minus the atomic binding energy of the photoelectrons.

A non-homogeneous group of electrons will be created by Compton scattering and pair production. Compton electrons scattered in the direction of the incident gamma ray will have an energy equal to $\frac{2\alpha}{1 + 2\alpha}$ times the incident gamma ray energy, where α is the incident gamma ray energy in units of mc^2 . A "back scattered" gamma ray will carry away the

¹²L. E. Glendenin, *Nucleonics* 2, No. 1, 12 (1948).

remaining energy. The forward scattered electrons will have more kinetic energy than those scattered in any other direction.

Pair production arises as the result of the "materialization" of a gamma ray. A high energy gamma ray in the vicinity of a nucleus may create an electron-positron pair. In this process both the electron and positron take up a minimum of $1 mc^2$ or 0.51 Mev each from the incident gamma ray because of their rest mass. Any additional energy possessed by the gamma ray over and above 1.02 Mev, which is the minimum required for pair creation, goes into imparting kinetic energy to the pair.

The energies of the secondary electrons produced in the above mentioned processes may be determined by absorption in aluminum or beryllium, by deflection of the electrons in electric and/or magnetic fields, from path lengths in a cloud chamber, or from the amount of fluorescence produced in certain crystals by the electrons.

Internal Conversion Electron Method

This method uses the same technique as that discussed above for the photoelectric process except that the internal conversion electrons emitted in the same nuclear transitions that produce the gamma rays are measured, whereas the photoelectrons are ejected by gamma rays striking a thin target of secondary material. The ratio of the number of K conversion electrons ejected to the number of L electrons ejected for a given nuclear transition is not as simply predicted as the ratio of K to L photoelectrons ejected from a secondary material by gamma rays resulting from the given nuclear transition. The K to L ratio for conversion electrons depends on the multipole order and the energy of the gamma transition giving rise to them. The relative intensities of two given gamma rays will usually be

quite different from the intensities of the conversion electrons arising from them, and it is only in cases where the internal conversion coefficients are known that reliable information about the relative intensities of gamma rays can be obtained from their accompanying conversion electrons.

Proportional and Scintillation Counter Method

This method has been used to obtain all the energy measurements presented in this dissertation. The method will be described in detail in the next chapter. In general it is less laborious and is less time consuming than the previously discussed methods, and generally the experimental set-up is less intricate.

CHAPTER II

APPARATUS

Proportional Counters

A study of electromagnetic radiation with proportional counters has been undertaken. A proportional counter generally consists of an axial wire (a few mils in diameter) in a glass and/or metal cylinder (a few centimeters in diameter). A large variety of gases can be used and at pressures ranging from a few mm Hg to many atmospheres in filling the cylinders. A proportional counter will provide an output voltage pulse which is proportional to the number of primary ions produced within the counter by the ionizing particle.

A study of the mechanism of proportional counters has been made by various authors,¹ and only a brief description will be presented here. Suppose an ionizing particle produces N primary ion pairs (electron and positive ions). The electrons will be impelled toward the center wire by the low electrostatic field ($E_r \propto 1/r$) which exists throughout most of the counter volume until they reach the immediate vicinity of the wire. In the very high field near the wire the electrons will gain sufficient energy from the field in one free path to ionize a gas atom. As soon as the ionization by collision starts, two electrons are in evidence -- the original one plus that liberated in the collision. These two electrons proceed

¹C. G. Montgomery and D. D. Montgomery, Phys. Rev. 57, 1030 (1940); M. E. Rose and S. A. Korff, Phys. Rev. 59, 850 (1941); and S. A. Korff and R. D. Present, Phys. Rev. 65, 274 (1944).

toward the wire, making further collisions. Since the field increases toward the wire, if any one collision is ionizing, all subsequent collisions are likely to produce ionization. Since two electrons are available after each collision there will be progressively more electrons produced as the initial one travels toward the wire, and an avalanche of electrons is said to have been formed.

According to the discharge mechanism stated above, a change in potential of the center wire will be produced by the inductive action of the positive ions as they cross the counter. The change in voltage may be calculated as follows. Let Q be the charge per unit length on the counter wire, and assume that there is a space charge sheath, of negligible thickness and of charge q per unit length, of positive ions at a distance r from the axis of the counter wire, extending for a length L along the counter. the wire potential, V , will be given by

$$V = \int_r^{r_c} \frac{2(Q+q)dr}{r} + \int_{r_w}^r \frac{2Q}{r} dr = \frac{Q}{c} + 2q \ln r_c/r \quad (10)$$

where r_c and r_w are the radii of the counter cathode and wire, respectively, and $c = (2 \ln r_c/r_w)^{-1}$ is the capacity per unit length of the counter. Let C_1 be the capacity of that portion of the wire not surrounded by the positive ion sheath, together with the other bodies attached to the wire, and let Q_1 be the total charge on them, from which it follows that $V = Q_1/C_1$. After the electrons which were formed in the counter have been collected (the mobility of electrons is much greater than that of positive ions, and it is assumed that all the electrons are collected on the wire before the positive ions have moved appreciably), the following relation exists between the charges.

$$QL + Q_1 = V_0(cL + C_1) - qL \quad (11)$$

Substituting the value of Q and Q_1 given above into equation 10 gives

$$\Delta V = V_0 - V = 2q \left[\frac{\ln r/r_w}{1 + (C_1/cL)} \right] \quad (12)$$

where ΔV is the change in potential of the center wire which was initially at a potential V_0 . Since $cL + C_1 = C$ is the capacity of the central wire and those portions of the detecting circuit connected electrically to it, ΔV may be expressed as follows.

$$\Delta V = \frac{qL}{C} \left[\frac{\ln r/r_w}{\ln r_c/r_w} \right] = \frac{Ane}{C} \left[\frac{\ln r/r_w}{\ln r_c/r_w} \right] \quad (13)$$

where A is the gas amplification and equals the total number of avalanche electrons reaching the center wire for each initial ion pair produced, and e is the charge of the electron. When all the positive ions have been collected (i.e., $r = r_c$) the output pulse from the counter will be equal to Ane/C . The time required for the output pulse to reach maximum is $\sim 10^{-3}$ sec.

In order that the proportional counter will have a more rapid discharge rate, the output pulse is generally differentiated by a RC circuit with a time constant that is short compared to the collection time of the positive ions. This leads to a reduction in signal amplitude, but it is not a serious handicap since the gas amplification can be made quite large ($\sim 10^6$).

The gas amplification A depends on the wire radius, the capacitance of the system, the counter voltage, the pressure of the gas, and the kind of gas. Because the gas amplification is an exponential function of the

voltage, the high voltage must be kept constant in order to prevent any change in the gain occurring while measurements are being made with the counter. There is an inherent fluctuation in the size of output pulse due to the statistical nature of both the number of primary ion pairs produced and the gas amplification, but this variation is not large enough to impair the instrument's utility as an energy measuring device.

Rose and Korff² recommend the addition of a polyatomic constituent in order to stabilize the gas amplification. The effect of the polyatomic molecule is to suppress the liberation of electrons at the cathode by ultra-violet photons and by positive ion bombardment.

The low field region at either end of the counter must be kept at least one counter diameter away from the counting volume to prevent particles from entering this region. The dimensions of the counter must be large compared to the maximum path length of the ionizing particle in the sensitive volume. If an appreciable fraction of the primary electrons produced by the gamma ray dissipate only a portion of their total energy within the counter, the spectrum is distorted because such electrons would be recorded as having lower energy. Thus higher energy events make a larger counter necessary and this requirement limits the useful operating range of proportional counters. It is also essential that the counters have a maximum absorption of the incident radiation in the gas and a minimum absorption in the wall, since the photoelectrons released in the wall material will emerge with greatly reduced energies.

²M. E. Rose and S. Korff, Phys. Rev. 59, 850 (1941).

Sodium Iodide Crystal Detectors

Scintillation spectrometers can provide energy measurements over a much wider range than proportional counters and are also more sensitive, but at the present time they do not have as good resolution as proportional counters at the same energy.

Gamma rays interact with matter by the three well-known processes of Compton effect, photoelectric effect, and pair production. In the case of a NaI crystal with a small thallium impurity (about 0.05 per cent by weight), the photoelectric process is the predominant one for gamma rays having energy below 500 kev. A gamma ray detected by the crystal loses its energy in exciting and ionizing the molecules of the crystal. These molecules then radiate energy in the form of light which is the phenomenon upon which the operation of a scintillation counter depends.

A scintillation counter was built using a 1.5 inch diameter and 1 inch thick NaI crystal. The crystal was placed in a light tight 10 mil thick aluminum can and sealed with mineral oil to a lucite light piper. The light piper was fastened to a RCA-5819 photomultiplier tube with Canada balsam.

The photomultiplier consists of a photocathode, which converts a fraction of the photons falling on it into electrons, followed by a series of dynodes, each at a higher potential than the preceding one. Electrons photoelectrically emitted from the cathode are drawn to the first dynode; with a secondary emission ratio greater than unity, secondary electrons are emitted which, in turn, give rise to an amplified current at the next dynode. By the time the electron stream has reached the anode, the original photocurrent is amplified R^n fold, where R is the secondary

electron emission ratio, and n is the number of dynodes. For the case of a RCA-5819 tube which has 10 dynodes, an amplification factor of a million would not be difficult to obtain. Actually the number of secondary electrons produced at each dynode will vary in a statistical manner, so that the pulses are not all the same height. Morton and Mitchell³ have shown that the spread in pulses due to this statistical fluctuation is small compared to the spread in the original number of photoelectrons.

The size of the output pulse from a NaI counter is very closely proportional to the incident gamma ray energy over a wide range of energies according to Bell.⁴

Electronic Equipment

The output pulses from the detectors which were described earlier are transmitted to a Model A1 linear preamplifier (type B) and amplifier⁵ through a coaxial cable. After being suitably amplified, the pulses are then applied to the vertical plates of a DuMont type 248A cathode ray oscilloscope. Simultaneously a constant voltage pulse from the A1 amplifier initiates the oscilloscope sweep circuit, so that all observed pulses begin from the same spot on the oscilloscope screen. The sweep duration is set for approximately 5 microseconds. In order to obtain permanent records and to make better analysis of radiation spectra, time exposure

³G. A. Morton and J. A. Mitchell, *Nucleonics* 4, No. 1, 16 (1949).

⁴P. R. Bell, *Science* 112, 7 (1950).

⁵W. H. Jordan and P. R. Bell, *Rev. Sci. Inst.* 18, 703 (1947).

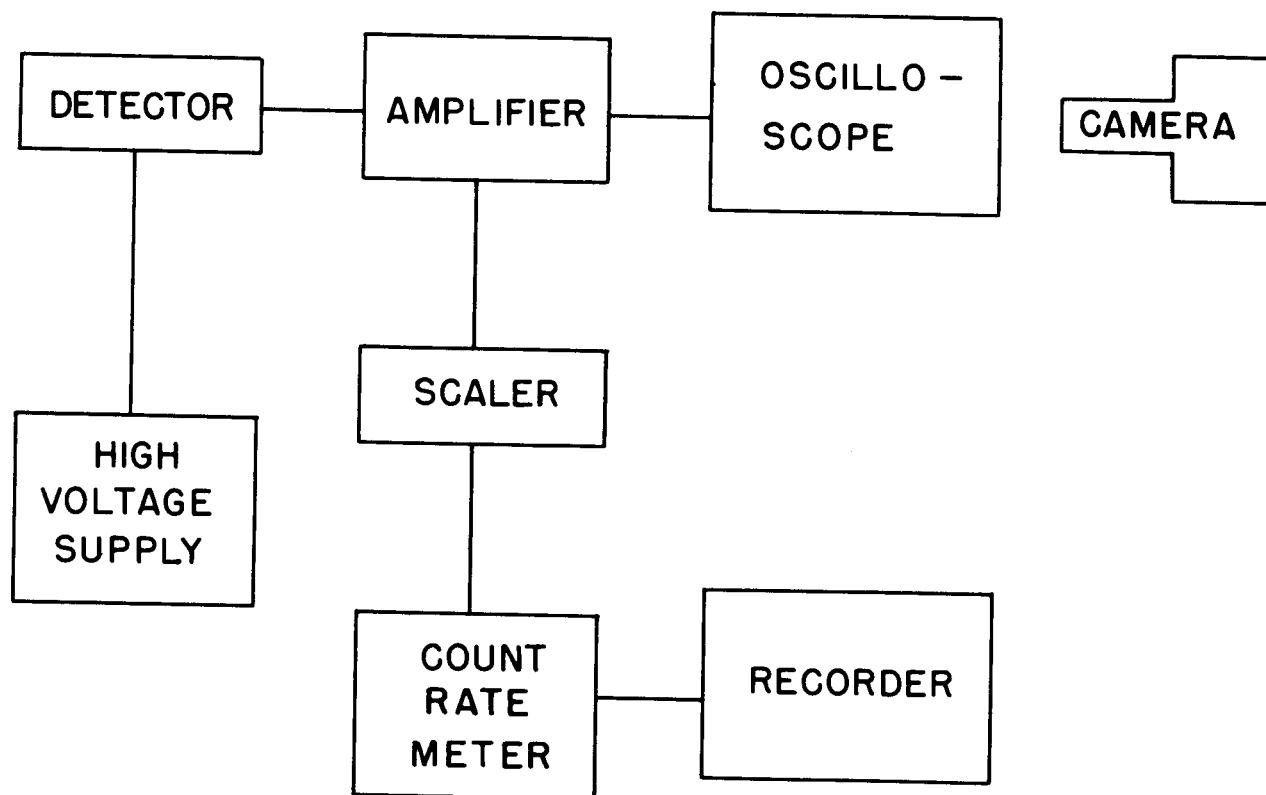


FIG. 1
BLOCK DIAGRAM OF SPECTROMETER

photographs with a 35 mm DuMont Oscillograph Record Camera were taken of the spectra as displayed on the oscilloscope screen. A type P11 screen was selected for the oscilloscope tube due to its short persistence and its good photographic qualities.

All photographs were made using Ansco Supreme film and developed in Kodak D-19 developer for seven minutes at 20°C. The films were scanned with a recording microphotometer built by Dr. Max Goodrich. This transposed the photographic data into quantitative form.

The output from the Al amplifier was also connected to an Atomic Instrument Company model 101-A scaler to which a register could be connected in order to measure the counting rate. For convenience, however, a logarithmic count rate meter and a recording potentiometer were connected to the scaler output. This made it possible to obtain a decay curve of the radioactive nuclei being examined. A block diagram of the entire circuit is shown in Fig. 1.

Preparation of Samples

All the radioactive nuclei were produced by neutron irradiation within the Oak Ridge pile through the use of the fast pneumatic tube facilities designed by Dr. Edward C. Campbell. A small sample of the order of 25 mg/cm² of the material to be investigated (usually an oxide or powdered metal) is stuck between two Scotch cellophane tape disks 9/16 inch in diameter. The sample is fastened in a nylon "rabbit" prior to its trip into the pile. The nylon "rabbit" is essentially a small block of nylon (1.125 x 0.835 x 0.330 inches) with a cylindrical hole, whose axis is

parallel to the small dimension, into which the sample is inserted. The "rabbit" runs through an aluminum tube (1 x 1/2 inch) powered by compressed carbon dioxide when going back and forth into the pile. The one-way trip takes less than 1/3 second. The sample usually remains in the pile between one second and one minute depending upon its cross-section and half-life. Upon withdrawal from the pile the "rabbit" is stopped in a lucite section of tubing which is transparent to gamma radiation, and by having the detector placed near the stopping position of the "rabbit", observation of the gamma radiation may be begun immediately after the sample is brought out of the pile. For nuclei with half-lives of the order of a minute or longer, the sample may be removed from the tube and "rabbit" before observing the radiation. This procedure eliminates the background due to the "rabbit" and any contamination from the pile which might have accumulated in the tube. A better geometry is also obtainable since the sample can be placed nearer to the detector by removing it from the pneumatic tube before examining the radiation.

CHAPTER III

EXPERIMENTAL RESULTS

Preliminary Tests

The first attempt in the present research to detect low energy gamma rays (< 50 kev) was made using an argon-methane filled proportional counter designed similar to the one used by Bernstein and others¹ at Brookhaven National Laboratory. Brass tubing 12 inches long and 4 inches in diameter was used to make the counter shell. The center wire is 4 mil tungsten; it is supported by a Kovar seal at one end and is fastened rigidly to the copper plate which seals the counter at the other end. A glass bead insulator was inserted in the center wire about 2 inches from the end plate in order to isolate the high potential from the shell. Heavy leads were brought in at least 2 inches to prevent field distortion at the counter ends. A 30 mil thick beryllium window is mounted in the side of the counter to admit radiation into the sensitive volume. The counter is filled to atmospheric pressure with a mixture of 90% argon and 10% methane. The preamplifier is connected rigidly to the counter to provide electrostatic shielding and to remove the need for a cable between them. The counter is operated with a positive 2500 volts applied to the center wire and with the shell or cathode grounded, which is advantageous from a safety standpoint.

¹W. Bernstein, H. G. Brewer, Jr., and W. Rubinson, *Nucleonics* 6, No. 2, 39 (1950).

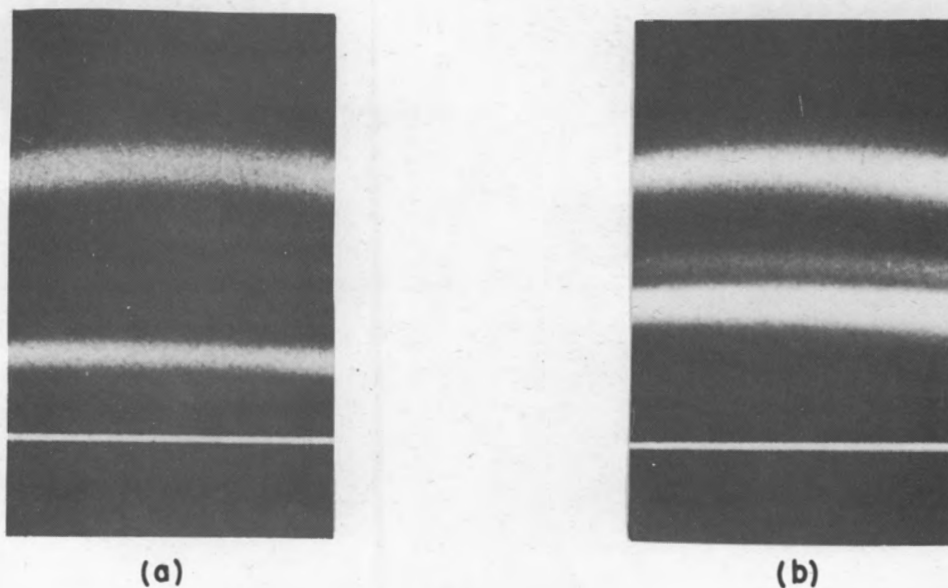


FIG. 2. Sb^{122} (a) K XRAYS DETECTED WITH THE ARGON COUNTER; (b) K XRAYS DETECTED WITH THE KRYPTON COUNTER.

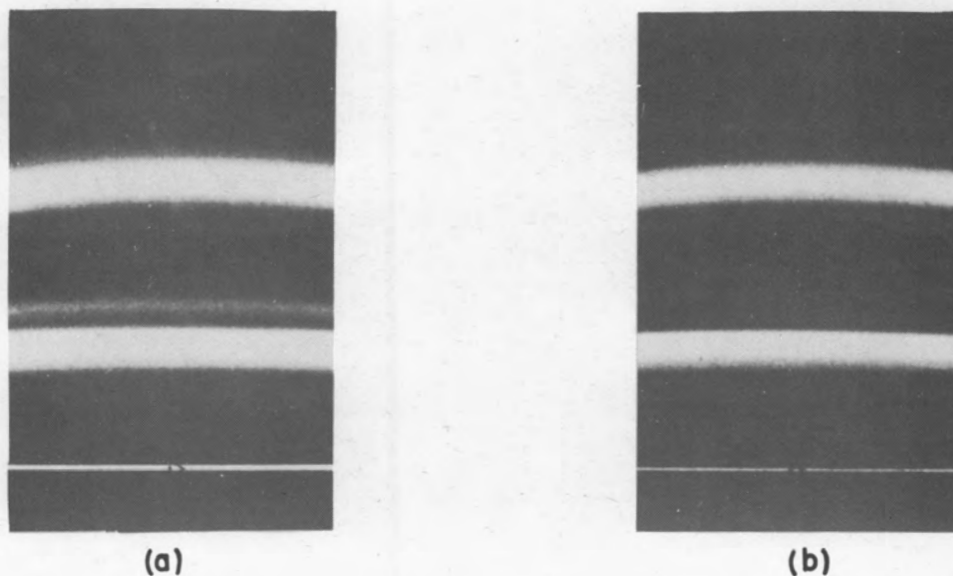


FIG. 3. Cd^{109} (a) K XRAYS DETECTED WITH THE KRYPTON COUNTER; (b) K XRAYS DETECTED WITH THE KRYPTON COUNTER WITH PALLADIUM ABSORBER.

Fig. 2a shows the x-rays from Sb^{122} as detected with this counter. A sample of isotopically enriched Sb^{121} was irradiated in the pile for one minute, and this photograph was taken while the sample decayed. The total exposure time amounted to one minute and began immediately after the sample was removed from the pile.

According to der Mateosian and Goldhaber², Sb^{122} has a metastable state which decays with a 3.5 minute half-life by emitting a 68 kev gamma ray (more will be said about this point later). It is to be expected that this gamma ray is internally converted. Immediately following the emission of conversion electrons, x-rays characteristic of the shell from which the electrons came should be emitted due to the existing vacancy in the electron shell.

The picture shown in Fig. 2a was made with a lucite absorber placed in front of the counter window in order to stop all beta radiation and Auger electrons. The top line shown is due to the Sb K x-ray, and the lower line is the Cu K x-ray caused by the fluorescent radiation produced in the counter walls by the antimony x-rays. The efficiency of the counter as a function of the energy of the incident radiation is too low to detect the 68 kev gamma ray, and the Sb L x-rays are too soft to penetrate the lucite absorber. The total number of pulses registered in making this photograph was over fifty thousand.

During a discussion with Dr. C. J. Borkowski about various details concerning some of my results with the brass counter, he suggested that I use a thin wall Eck and Krebs type counter which he developed and has been

²E. der Mateosian and M. Goldhaber, Phys. Rev. 82, 115 (1951).

using quite successfully. One big advantage of this type of counter over the brass one that I had built is its much smaller size. Because of the high background prevalent in the vicinity of the pile, this new counter could be much more easily shielded. Actually, it was possible to eliminate the radiation shielding altogether in most cases. To a first approximation, the background counting rate is proportional to the sensitive volume of the proportional counter. The brass counter has roughly 25 times the volume of the glass type counter, and its background counting rate is larger by a similar factor, but this disadvantage can be compensated for with sufficient shielding. Stray radiation from the source under investigation, however, will ionize the shielding material which will then emit fluorescent x-rays characteristic of this material. These x-rays are readily detected by the counter, and they are often difficult to distinguish from the x-rays emitted by the true source.

Fig. 2b shows the x-rays from Sb^{122} as detected with a thin wall Eck and Krebs type counter filled with 60 cm krypton and 6 cm methane. The counter is made from 19 mm O.D. glass tubing with 5 mil wall upon the inside of which a thin layer of silver is deposited to serve as the cathode. The overall length of the tube is 8 inches with the counting region confined to the central 3 inch section. As a protective covering and for electrostatic shielding the glass tube is enclosed in a one inch O.D. aluminum tube in which a window is provided for the admission of radiation. A 4 mil center wire of tungsten is the anode which operates at approximately 2100 volts. This counter is likewise connected directly to a pre-amplifier.

The top line in Fig. 2b shows the Sb K x-ray just as in Fig. 2a in the case of the argon counter. The double line appearing in the middle

of Fig. 2b has a different origin from any line shown in Fig. 2a. Whenever an Sb K x-ray produces a photoelectron from the K shell of krypton, there are two possible events that can occur. The ionized krypton atom will either emit an Auger electron or its own characteristic K x-ray. If the Auger process occurs, the entire energy of the incident x-ray is spent in the counter, and this produces a pulse whose height is equivalent to the incident K x-ray energy. If a K x-ray is emitted by the krypton, it has a good probability (~ 90 per cent) of escaping from the counter and thus part of the energy of the incident x-ray is lost. This accounts for the double line shown in Fig. 2b where the fainter line is due to the K_{β} radiation of antimony minus the krypton K x-ray energy (13 kev) and the heavier line is due to the K_{α} radiation of antimony minus the krypton K x-ray. This point will be proven shortly. The resolution of this instrument as measured by the ratio of the peak width at one-half maximum intensity to the peak energy is 14 per cent. This is not sufficient to differentiate between the K_{α} and K_{β} lines of antimony directly, but when a constant energy is subtracted from the incident K radiation (due to the escape of a krypton K x-ray), the percentage-wise difference between the K_{α} and K_{β} lines is increased and they are resolved as shown in Fig. 2b. It should be pointed out that following the emission of a K x-ray in the krypton there may be L, M, etc. x-rays emitted as well as Auger electrons from these shells, but these are readily absorbed within the counter. Likewise, in the event that the photoelectron comes from outside the krypton K shell, any subsequent radiation is absorbed in the counter, and this produces a pulse whose height is equivalent to the energy of the incident radiation. The total number of pulses registered in making the photograph

shown in Fig. 2b was about a hundred thousand.

As in the case of the argon counter, the efficiency was too low to detect any unconverted 68 kev gamma rays and the antimony L x-rays failed to penetrate the lucite absorber which is needed to stop the beta rays. In the case of the thin wall glass counter there is no evidence of any fluorescent x-rays from the counter walls. With the argon counter, apparently no appreciable fraction of the argon K x-rays escape, which could be due to the larger size of the counter. However, the resolution is probably too poor to detect the less energetic line which would result if a K x-ray of argon did escape, since this line would differ in energy by only 3 kev from the total energy available (26 kev).

Fig. 3 shows the x-rays from 330 day Cd^{109} as detected by a krypton proportional counter. According to Bradt and others,³ Cd^{109} decays by K capture to an isomeric state of Ag^{109} which subsequently emits a 89 kev gamma ray that is highly converted and has a half-life of 39 seconds. Since the K capture process leaves a vacancy in the K shell and at the same time the nuclear charge has decreased by one unit, K x-rays characteristic of the daughter element will be emitted as the missing K electron is replaced in order to render the atom electrically neutral. Thus both the K capture process and the internal conversion process give rise to silver x-rays in the decay of Cd^{109} . In Fig. 3b a palladium absorber has been inserted between the Cd^{109} source and the krypton counter. The K absorption edge of palladium is at 24.4 kev and any radiation slightly more

³H. Bradt, P. C. Gugelot, O. Huber, H. Medicus, P. Preiswerk, P. Scherrer and R. Steffen, *Helv. Phys. Acta* 20, 153 (1947).

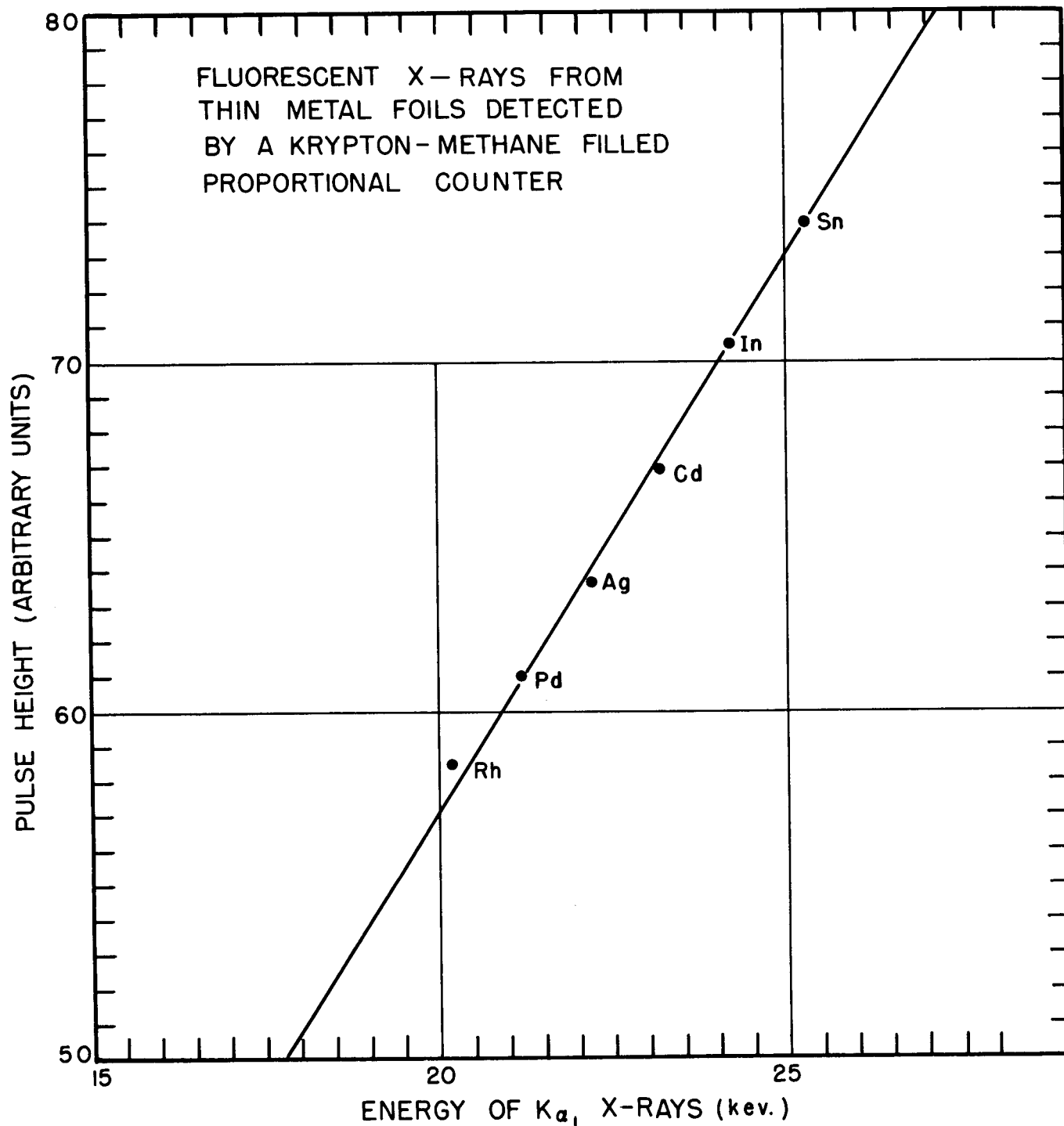


FIG. 4

energetic than this will be strongly attenuated while slightly less energetic rays will suffer little attenuation. The K_{β} x-rays of silver have an energy of 25.0 kev and are clearly seen to be strongly absorbed by the palladium; whereas, the K_{α} x-rays of silver have an energy of 22.2 kev and are transmitted. Fig. 3b was given three times the exposure of Fig. 3a in order to give comparable intensities to the two photographs.

Calibration of the Proportional Counter Spectrometer

A typical energy calibration of the krypton counter is shown in Fig. 4. Fluorescent x-rays from thin metal foils excited mainly by the x-rays emitted from radioactive Eu^{152} (9.2 hour half-life) were used as x-ray sources.⁴ The beta particles from the Eu^{152} were absorbed with a one centimeter thickness of beryllium which has a good transparency for the x-rays. The hard gamma rays emitted were not bothersome as the counter efficiency was too low to detect them. The x-rays from europium, after penetrating the beryllium absorber, were allowed to fall on a thin sheet of the appropriate element which was placed in front of the counter window. Some europium x-rays penetrated the radiator element, but these were not sufficient to mar the photographs that were made of the fluorescent x-rays. This method proved much more satisfactory than the use of an x-ray machine which had been previously tried. It was difficult to obtain low enough intensities with an x-ray machine, and there was always a continuous background of white radiation in addition to the characteristic lines sought.

⁴G. M. Inch, *Phil. Mag.* 41, 857 (1950).

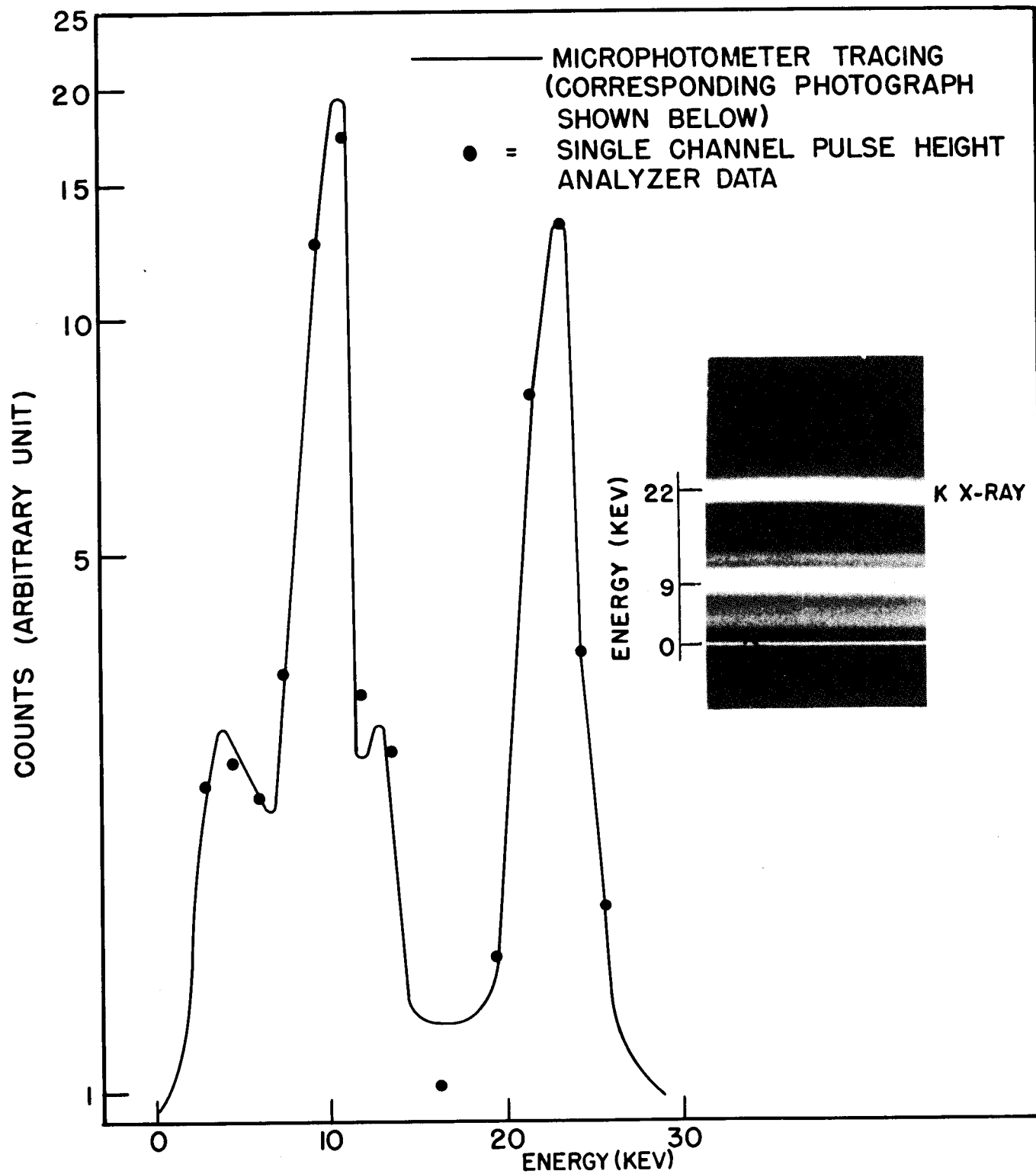


FIG. 5
X-RAYS FROM Cd^{109} (330 d) AS DETECTED BY KRYPTON
METHANE FILLED PROPORTIONAL COUNTER

In order to determine the accuracy of the intensity measurements obtained from the films, a series of exposures to the same source for various periods of time were included in the films. A plot on log-log graph paper of the film opacity (the reciprocal of the transparency relative to the blank film) as measured by the microphotometer, versus the exposure time resulted in a straight line with a slope of one provided that the opacity was not less than 3 nor more than 30. In order to make relative intensity measurements outside of this range, corrections must be applied to the microphotometer readings.

As a further check on the accuracy of the film intensities, the microphotometer tracings were compared with the results obtained using a single channel pulse height analyzer.⁵

Fig. 5 shows the silver K x-rays emitted from 330 day Cd^{109} as detected with a krypton proportional counter. The division of the pulses between the two main peaks depends on the fluorescent yield of krypton and is independent of the incident radiation. The fluorescent yield of a given shell of an atom is defined as the ratio of the number of x-rays emitted in transitions to that shell to the number of vacancies formed in the shell. When a photoelectron is ejected from the K shell in the krypton counter, there are two different ways in which the vacancy may be filled; either a characteristic K x-ray is emitted when an electron falls in from a higher level or the corresponding energy is given to one or more Auger electrons ejected from higher electronic levels. The high energy peak observed in Fig. 5 is produced by the Auger process occurring

⁵E. Fairstein, A Sweep Type Differential and Integral Discriminator, ORNL-893, Series A (1951).

in the krypton counter, and the lower peak (actually a double peak) is produced when a krypton K x-ray escapes from the counter following the photoelectric process. The ratio of the area under the "escape" peak to the total area under both the "escape" and the full energy peak will give the fluorescent yield for the K shell of krypton if two corrections are made. The fraction of the total pulses in the "escape" peak was found by numerical integration to be 53 per cent.

The first correction to be made is due to the reduced intensity of the "escape" peak caused by the reabsorption of the K x-rays of krypton in the counter gas. The value for the mass absorption coefficient of krypton for its own K x-rays is $30 \text{ cm}^2/\text{gm}$ as given by Jönsson's "universal" absorption curve (see Compton and Allison⁶) which is claimed to be accurate to ± 5 per cent in most cases. This value is confirmed by the following formula due to Walter (see Compton and Allison⁷) based on a summary of the experimental data available on x-ray absorption.

$$\mu = \frac{5.13 \times 10^{-4} Z^{4.30} \lambda^3}{A} \quad (14)$$

where

μ = mass absorption coefficient for incident x-rays.

Z = atomic number of the absorbing material.

λ = wave length in Angstroms of incident x-rays.

A = atomic weight of the absorbing material.

⁶ A. H. Compton and S. K. Allison, X-rays in Theory and Experiment (New York: D. Van Nostrand Co., Inc., 1935) p. 540.

⁷ Ibid., p. 537.

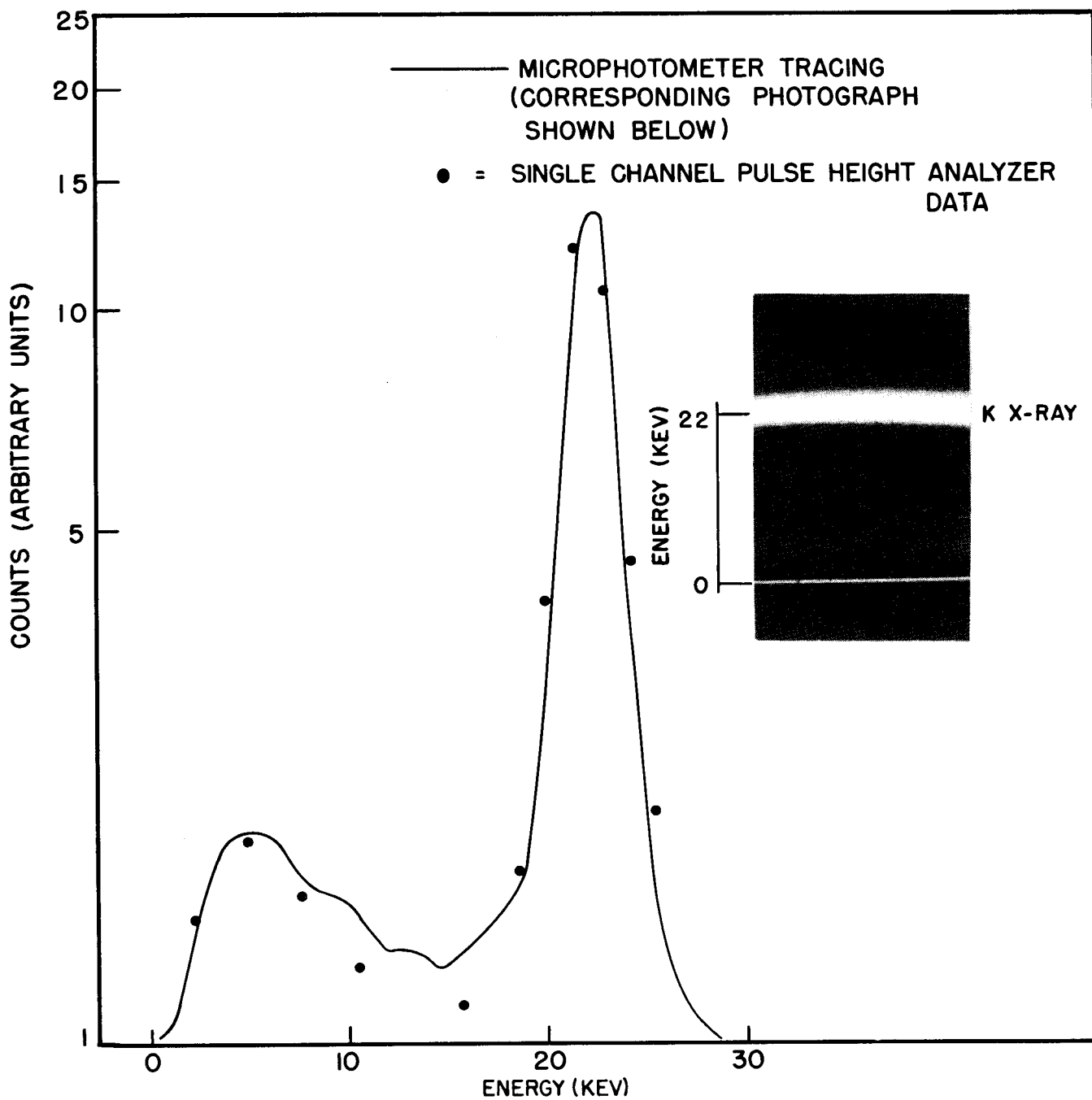
This formula applies only to wave lengths between the K and L absorption edges of the absorbing element. The mass absorption coefficient of krypton for its own K x-rays is

$$\mu = \frac{5.13 \times 10^{-4} (36)^{4.30} (0.98)^3}{83.7} = 28.3 \text{ cm}^2/\text{gm} \quad (15)$$

A value for the mass of krypton per square centimeter as seen by the krypton x-rays is not easily calculated because of the counter geometry and the complex spacial distribution of the fluorescent krypton radiation. An absorber thickness equal to the counter diameter (1.8 cm) \pm 25 per cent should be a valid assumption. For krypton at a pressure of 60 cm Hg and 24°C this gives a value of $4.8 \pm 1.2 \text{ mg/cm}^2$ for the average thickness of the krypton gas as seen by the krypton x-rays.

Substituting in the well known absorption formula $(1 - e^{-\mu x})$ gives 13 ± 3 per cent as the fraction of the krypton K x-rays absorbed within the counter.

A second correction is necessary to account for the incident radiation absorbed in the L, M, shells. Since approximately the total energy of the incident x-ray is then spent in the counter, this process cannot be distinguished from K absorption with subsequent emission of an Auger electron. The ratio of the absorption in the K, L, M, shells to that in the L, M, shells is known at the K absorption edge for most elements, and it is assumed that the ratio is the same for energies not much greater than the K binding energy. For the case of krypton this value was calculated from an empirical formula due to Jönsson (see Compton and Allison⁷) since there are very few measurements of the x-ray absorption coefficient of krypton reported in the literature. Jönsson



X-RAYS FROM Cd^{109} (330 d) AS DETECTED BY
XENON-METHANE FILLED PROPORTIONAL COUNTER

finds that the magnitude of the K absorption jump is well represented by the ratio of the energies of the K and L_I electron states. Comparison with experimental results indicates that this relation is accurate to ± 5 per cent in most cases. For krypton this formula gives a value of 7.4 ± 0.4 for the absorption jump. It follows, therefore, that the absorption in the L, M, shells constitutes a fraction $(7.4 \pm 0.4)^{-1}$ or 13.5 ± 0.7 per cent. Absorption of x-rays in the methane was neglected, since it is very small compared with that in krypton.

These two corrections give the final value for the fluorescent yield for krypton as 0.70 ± 0.03 . This value agrees with that found by West and Rothwell⁸ (0.67) who used a similar method for determining the fluorescent yield. Auger⁹ measured the fluorescent yield for various gases by observing the abundances of Auger electrons in a large number of K ionizations revealed by the photoelectron tracks in a Wilson cloud chamber. If such a photoelectron track is observed, and has no associated track with it whose length corresponds to the ejection by a K series line quantum of an electron from an outer shell in the atom, this atom must have emitted a characteristic K x-ray. In 320 instances Auger found that 156 were accompanied by an electron arising from the internal conversion of one of the K lines, hence he obtained a fluorescent yield of 0.51 for the K shell in krypton.

Fig. 6 shows the x-rays from Cd^{109} as detected by a xenon counter. This counter is identical with the krypton counter previously described

⁸D. West and P. Rothwell, *Phil. Mag.* 41, 873 (1950).

⁹P. Auger, *Ann. de Phys.* 6, 183 (1926).

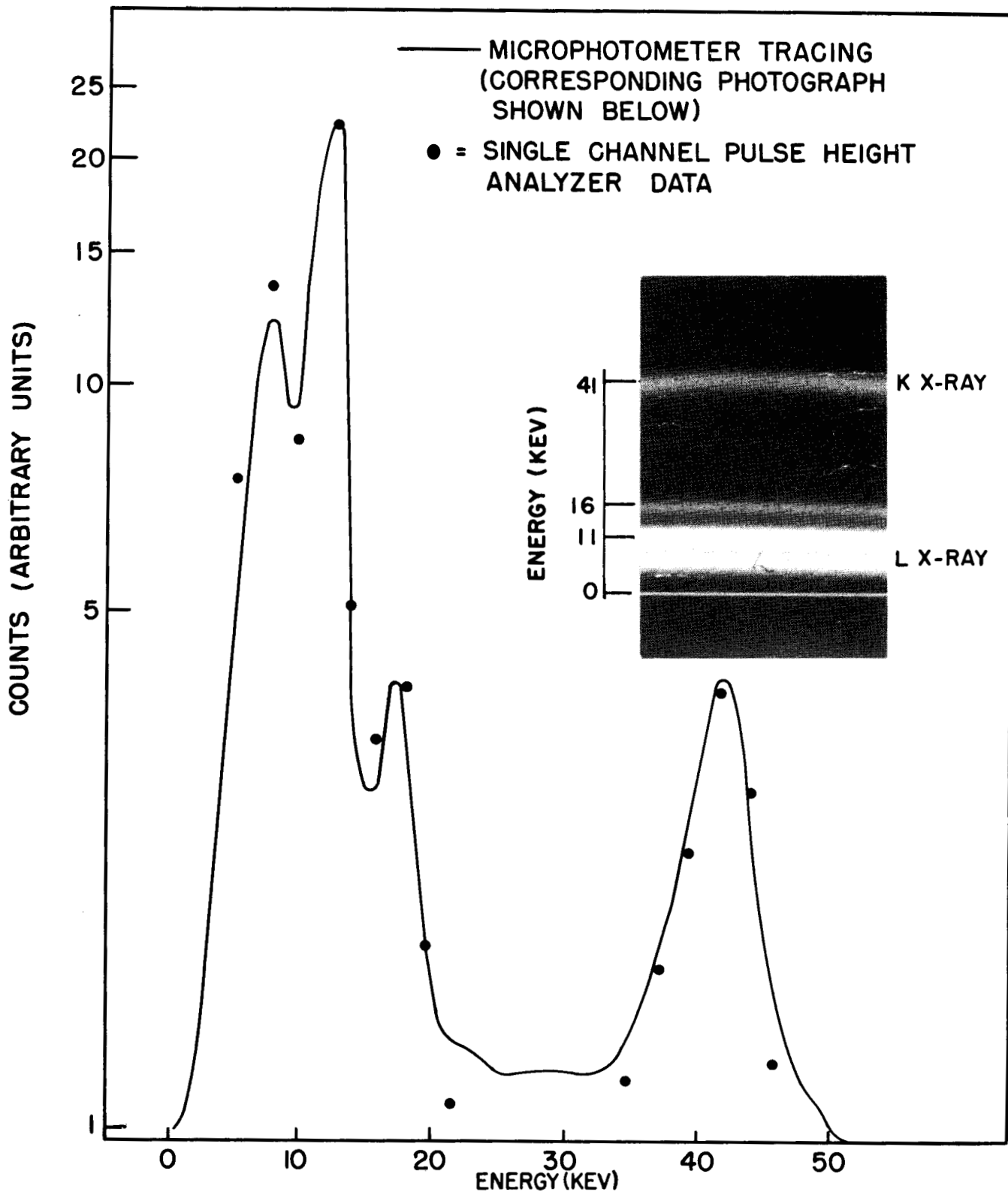


FIG. 7

X-RAYS FROM Eu^{152} (9.2 hr.) AS DETECTED BY
XENON-METHANE FILLED PROPORTIONAL COUNTER

except that it is filled with 60 cm Hg pressure of xenon and 6 cm Hg of methane. In the photograph there is only one line present, and this corresponds to the incident K x-ray energy. Since the radiation is not energetic enough to excite the xenon K x-ray (30 kev), it must be absorbed in the outer shells. Both the Auger electrons and the x-radiation that is subsequently emitted by the ionized xenon atoms are readily absorbed in the counter. This means that in the absorption process the total energy of the photoelectrons plus Auger electrons will be very close to the energy of the incident quantum.

Fig. 7 shows the x-rays from 9.2 hour Eu^{152} as detected by a xenon counter. The decay scheme of Eu^{152} has not been determined, but it is known that K capture occurs in addition to several beta and gamma transitions.¹⁰ One of the transitions is internally converted, but it is not known from what nucleus it arises. There are probably x-rays emitted during the decay of Eu^{152} other than the samarium K x-rays which follow the K capture process. A one centimeter thickness of beryllium was placed between the source and the counter in order to absorb all the beta rays. The peak at 41 kev is due to the absorption of the total energy of the incident K x-rays. As stated before, the resolution of the spectrometer is not sufficient to resolve the K_{α} and K_{β} x-rays directly. The peak at 11 kev is due to the incident K_{α} radiation and the subsequent escape from the counter of xenon K x-rays. The less intense peak at 16 kev results from the detection of the K_{β} radiation followed by the escape of the xenon K x-ray. The 6.5 kev peak is produced by the incident L x-rays

¹⁰J. M. Hill and L. R. Shepherd, Proc. Phys. Soc. A63, 126 (1950).

as the relative height of this peak is decreased by interposing a thicker beryllium absorber between the sample and the counter.

In a method analogous to that used for measuring the fluorescent yield of krypton, the fluorescent yield for the K shell of xenon was calculated, and it is found to have a value of 0.85 ± 0.5 . West and Rothwell¹¹ give a value of 0.81, and Auger¹² obtained a value of 0.71.

The pulse height analyzer data in the previous figures were superposed on the microphotometer tracings by normalizing the data so that the more energetic peak heights coincide. It should also be pointed out that the "counts" or ordinates are plotted to a logarithmic scale.

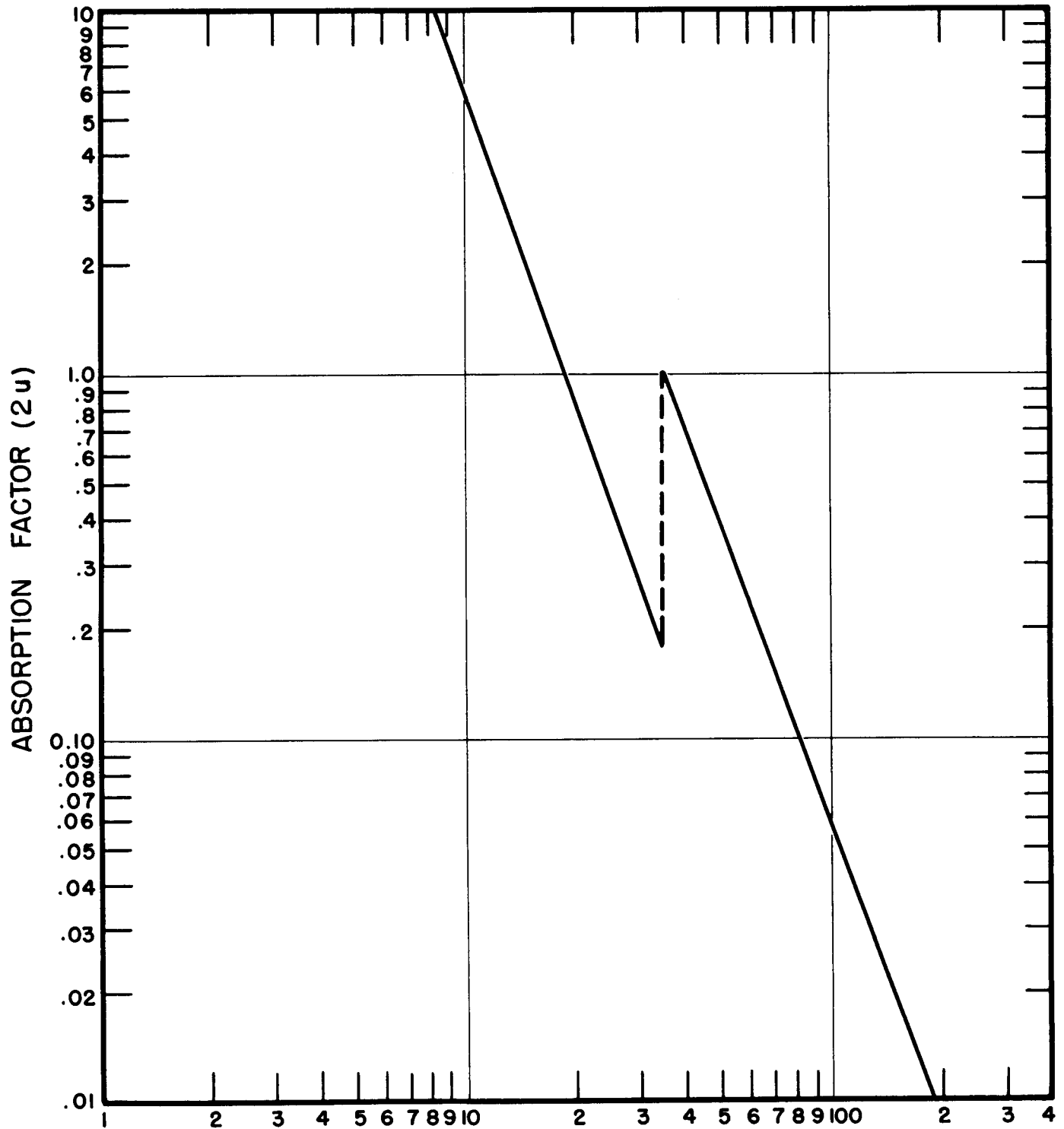
Counter Efficiency

In order to measure the counting efficiency of the xenon proportional counter described earlier as a function of the energy of incident radiation, a second counter was obtained which is identical to the first except it was filled to only one-half the pressure of the first. Counter 1 is filled to a pressure of 60 cm Hg of xenon and 6 cm Hg of methane, and counter 2 is filled to a pressure of 30 cm Hg of xenon and 3 cm of methane. The counting rates minus the background rates for the two counters were compared using the same x-ray source. This comparison was made using Cd^{109} and Eu^{152} which emit x-rays of energy 22 and 41 kev respectively.

The well known absorption formula gives as the ratio R for the

¹¹West and Rothwell, loc. cit.

¹²Auger, loc. cit.



ENERGY OF INCIDENT RADIATION (kev.)

FIG. 8

ABSORPTION CURVE FOR XENON COUNTER

counting rates of the two counters

$$R = \frac{I_2}{I_1} = \frac{I_0(1 - e^{-u})}{I_0(1 - e^{-2u})} = \frac{1 - e^{-u}}{e^{-u}(e^u - e^{-u})} \quad (16)$$

where I_2 is the counting rate of counter 2, I_1 is the counting rate of counter 1, I_0 is the intensity of the incident radiation, and u is the mass absorption coefficient of counter 2 for the incident radiation times the path length of the radiation in counter 2. Since counter 1 is filled to twice the pressure of counter 2, it has twice the path length of counter 2 for the incident radiation, hence the factor of 2 in the exponent.

$$\therefore u = \ln \left[\frac{R}{1 - R} \right] \quad (17)$$

R was found to be 0.576 and 0.579 in the case of Cd^{109} and E^{152} respectively. This leads to a value for $2u$ (the absorption factor for the higher pressure counter) of 0.62 and 0.64 for 22 and 41 keV radiation respectively. Any L x-rays emitted by the above sources were cut out by biasing the Al linear amplifier sufficiently. The two points are plotted in Fig. 8 and the lines are obtained by making their slope the same as that for the absorption coefficient of iodine which is a neighboring element that has been previously investigated (see Compton and Allison¹³). The K absorption edge for xenon (35 keV) was obtained from well known x-ray data. This is the point where the absorption coefficient of xenon abruptly changes because of ionization commencing in the K shell of xenon.

¹³Compton and Allison, op. cit., p. 801.

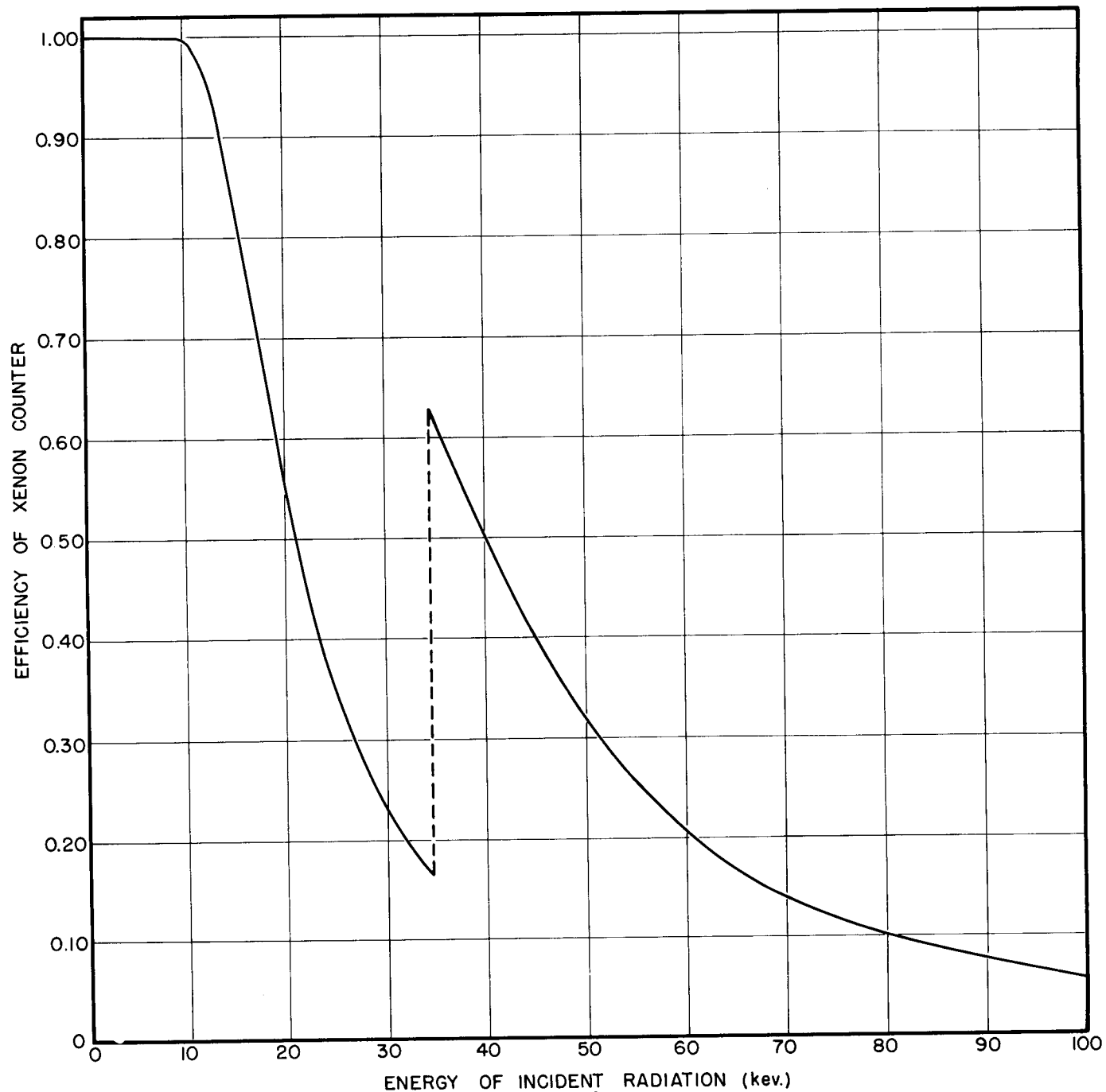
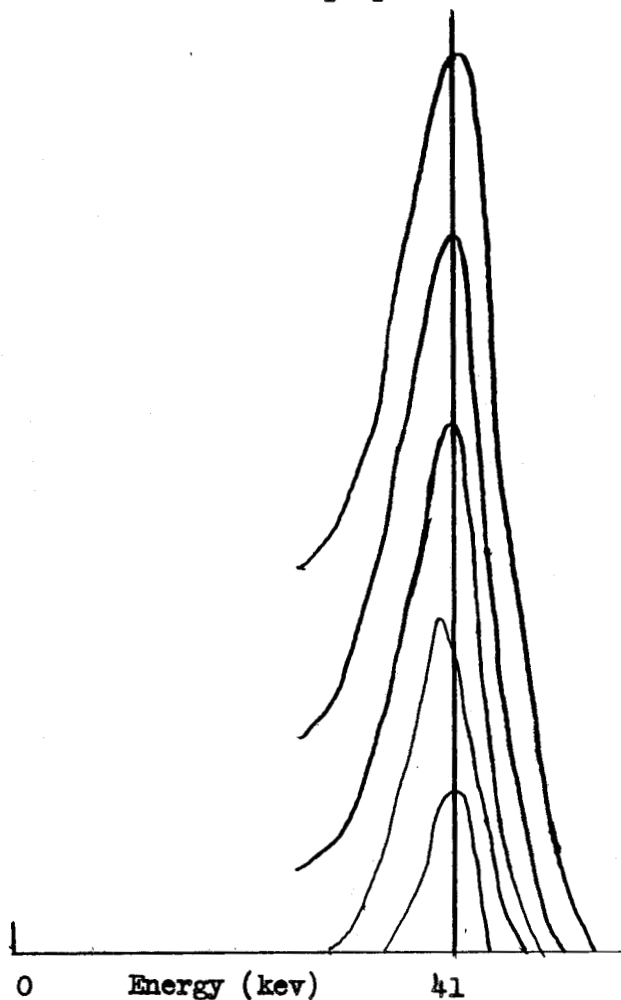


FIG. 9
EFFICIENCY OF XENON COUNTER AS A FUNCTION OF
 γ AND X RAY ENERGY

Fig. 9 gives the actual efficiency (neglecting geometric effects) of the xenon proportional counter ($1 - e^{-2u}$) as a function of energy of the incident electromagnetic radiation. For energies less than 5 kev, the absorption of the incident radiation by the counter walls becomes important, so for energies in this region Fig. 9 does not apply.

Accuracy of Energy Measurements

The following diagram shows a portion of the microphotometer traces from five separate photographs made of the x-rays emitted from 9.2 hour Eu^{152} as detected with a xenon proportional counter. The peaks represent



the energy of the incident x-rays (41 kev). Exposures times range from 5 to 80 seconds with any given curve resulting from twice the exposure time of the next lower curve.

The greatest fluctuation in peak position from the mean value (denoted by vertical line) occurs in the second from the bottom curve in the diagram. This deviation amounts to approximately 3 parts in 120 or 2.5 per cent which is assumed as the limits of accuracy for the energy measurements made with the proportional counter. This error of 2.5 per cent is about twice the probable error predicted by probability theory in the case of the five measurements presented above. It is felt that the wider limits placed on the accuracy are necessary in order to account for any systematic errors which may occur.

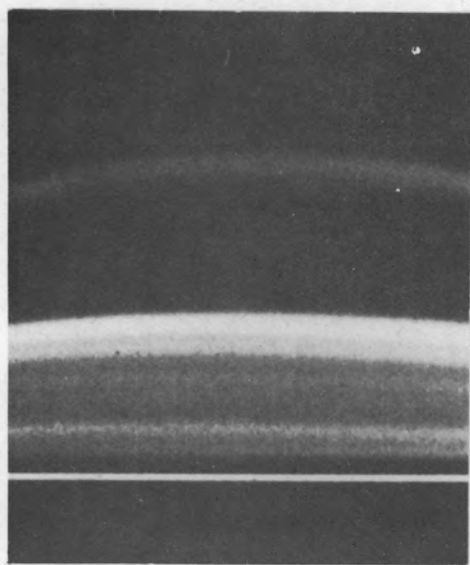
In the event that two gamma rays differing in relative energy by an amount less than 15 per cent are measured simultaneously, the error in the resultant energy measurement will in this case, no doubt, be greater than ± 2.5 per cent. This is due to the fact that the two gamma rays would not be resolved by the counter.

Gamma and X-ray Spectra of Various Short Period Activities

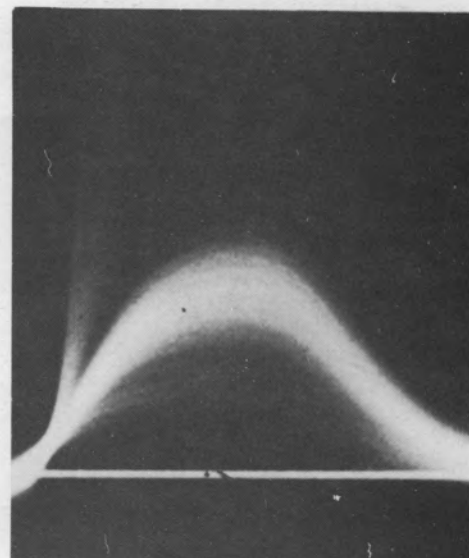
The results of a study of the electromagnetic radiation emitted by various short period radioactive nuclei are collected below.

10.7 Minute Co⁶⁰ Activity

The 10.7 minute period in cobalt produced by neutron irradiation



(a)

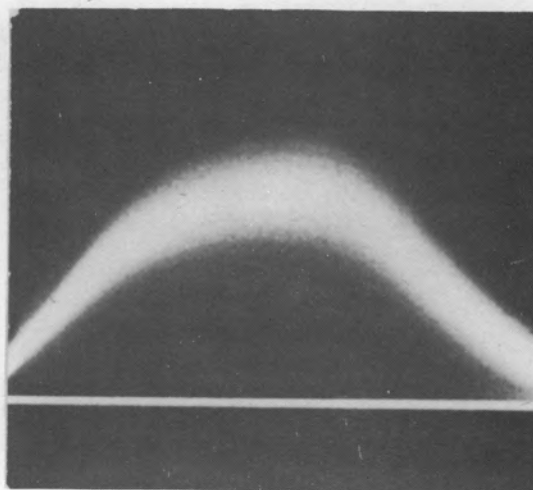


(b)

FIG. 10. Co^{60} (a) γ RAY AND K XRAY DETECTED WITH THE Xe COUNTER; (b) γ RAY DETECTED WITH THE NaI COUNTER.



(a)



(b)

FIG. 11. Se^{77} (a) K XRAY DETECTED WITH THE ARGON COUNTER; (b) γ XRAY DETECTED WITH THE NaI COUNTER.

of cobalt metal has been investigated by Deutsch and others.¹⁴ They report that at least ninety per cent of the disintegrations are by an isomeric transition of energy 56 kev, presumably to the five year level. The remaining ten per cent of the disintegrations are by a beta ray of 1.25 Mev followed by a single gamma ray of energy 1.50 Mev. Caldwell¹⁵ investigated the conversion electrons using a permanent magnet beta-ray spectrograph. He reports three conversion electron lines which were assigned to K, L, and M conversions of a single gamma ray of energy 58.9 ± 0.5 kev.

Fig. 10 shows the gamma rays from Co^{60} as detected by a xenon filled proportional counter (10a) and by a NaI scintillation counter (10b). Comparing the height of the gamma ray line in Fig. 10a to the distance from it to the "escape" line (29.7 kev below the gamma ray line due to the escape of a xenon K x-ray from the counter) gives an energy value of 58.5 ± 1.5 kev for the gamma ray.

The K x-ray of cobalt is faintly visible near the bottom of the photograph. These x-rays are emitted subsequent to the internal conversion process.

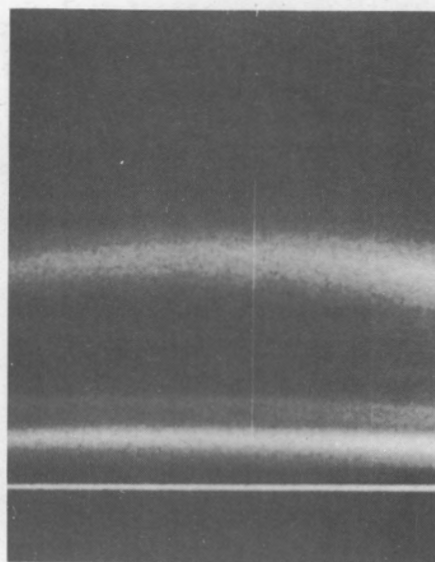
17.5 Second Se^{77} Activity

The 17.5 second period in selenium produced by neutron irradiation has been studied by Arnold and Sugarman.¹⁶ They found a gamma ray having

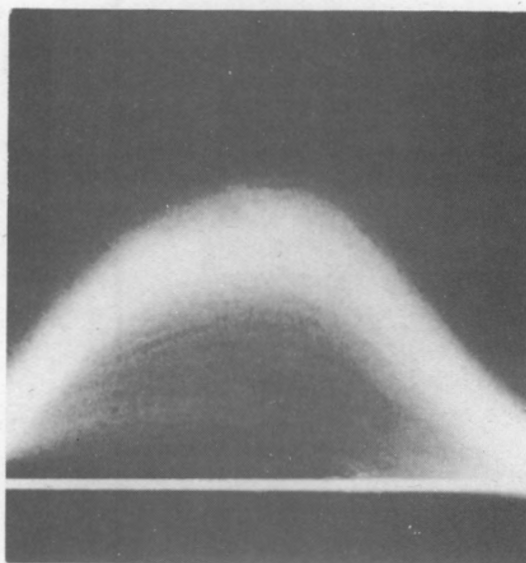
¹⁴M. Deutsch, L. G. Elliott and A. Roberts, Phys. Rev. 68, 193 (1945)

¹⁵R. L. Caldwell, Phys. Rev. 78, 407 (1950).

¹⁶J. R. Arnold and N. Sugarman, J. Chem. Phys. 15, 703 (1947).



(a)



(b)

FIG. 12. Zr⁹⁰ (a) K XRAY DETECTED WITH THE
Kr COUNTER; (b) γ RAY DETECTED WITH
THE NaI COUNTER.

an energy of roughly ~ 150 kev as determined from absorption measurements. Goldhaber and Muehlhause¹⁷ assigned this period to Se^{77} by observing the (n,γ) reaction in enriched Se^{76} .

Fig. 11 shows this gamma ray as detected by a NaI counter and also the K x-rays as detected with an argon filled proportional counter. The gamma ray in Fig. 11b has an energy of 130 ± 7 kev. This value was obtained by comparing the peak height shown with that obtained from the 279 kev gamma ray emitted by Hg^{203} . The error is assumed to be twice that used for the proportional counter measurements.

The double line shown in Fig. 11a results from the selenium K x-rays following internal conversion and the fluorescent x-rays of copper produced in the counter walls by the selenium radiation.

5 Second Zr Activity

An attempt was made to verify the 5 second zirconium (n,γ) reaction reported by Ageno.¹⁸ Because of the impurity of the zirconium source that was used, it is not known whether the gamma ray shown in Fig. 12b is emitted by zirconium or by a hafnium impurity. This gamma ray has a value of 188 ± 20 kev as determined by comparison with the 279 kev gamma ray of Hg^{203} . Hf^{179} is known to have a gamma ray whose energy is 220 ± 10 kev (see page 62), and this gamma ray is undoubtedly contributing to the peak shown in Fig. 12b.

¹⁷M. Goldhaber and C. O. Muehlhause, Phys. Rev. 74, 1248 (1948).

¹⁸M. Ageno, Nuovo Cimento 1, 33 (1943).

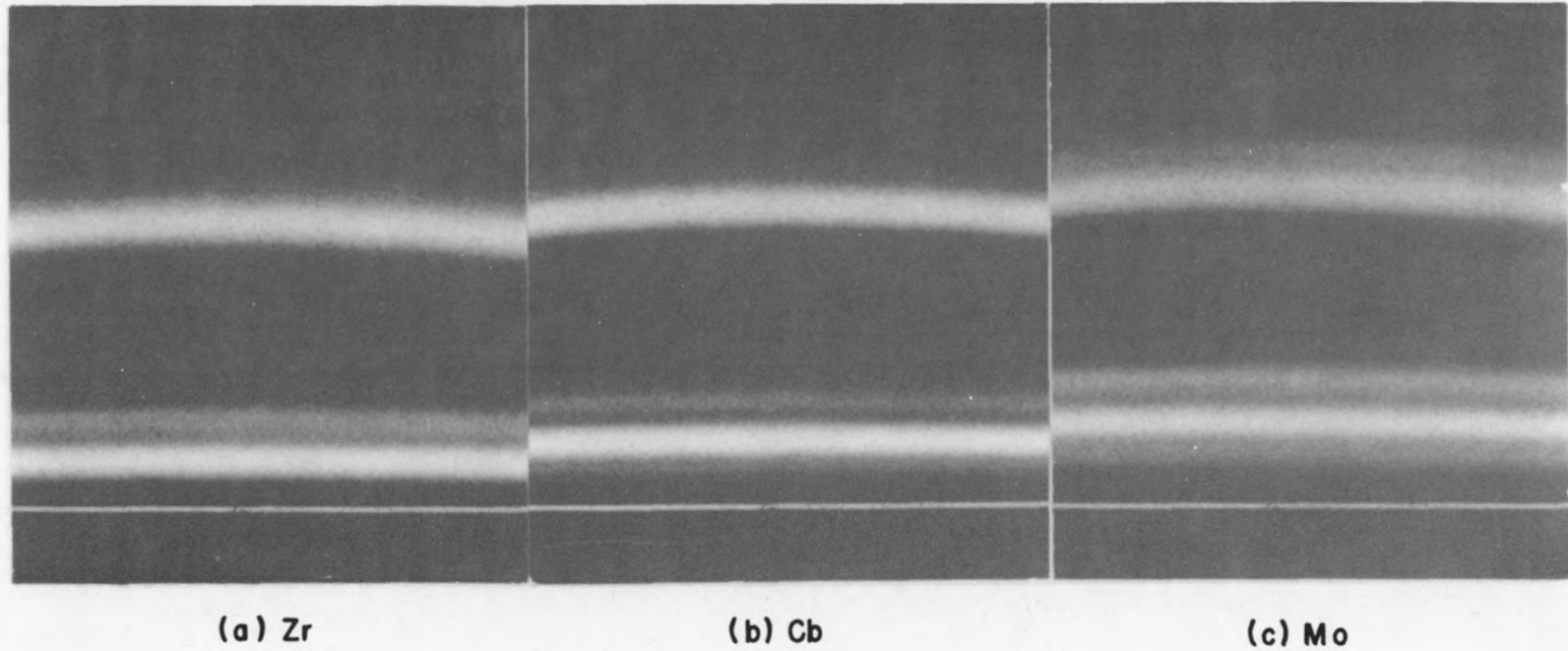


FIG. 13. K X RAYS FROM NEIGHBORING ELEMENTS DETECTED WITH THE KRYPTON COUNTER. (a) FLUORESCENT SOURCE; (b) RADIOACTIVE SOURCE; (c) FLUORESCENT SOURCE.

Fig. 12a shows the zirconium K x-rays as detected by a krypton proportional counter. These x-rays either could result from internal conversion occurring following an isomeric transition of the zirconium nucleus, or could be fluorescent x-rays from zirconium that has been ionized by the hafnium radiation.

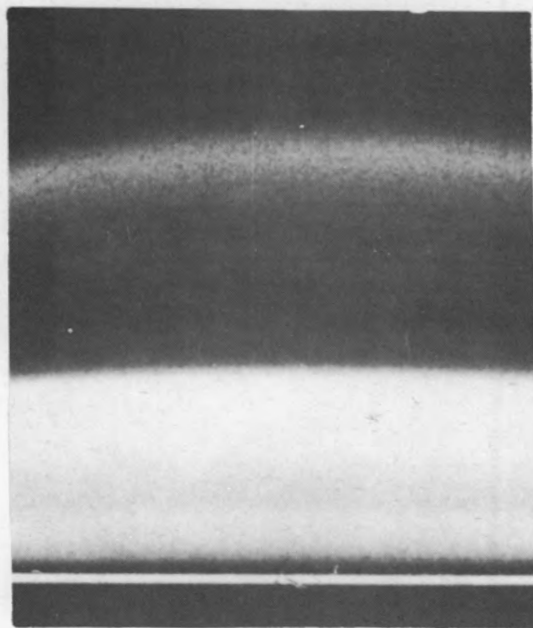
6.6 Minute Cb^{94} Activity

Goldhaber and Muehlhause¹⁹ report that very pure columbium exposed to slow neutron irradiation emitted strong K x-rays. By critical absorption they showed these x-rays to be characteristic K radiation of columbium which implies that they arise from an isomeric transition in columbium. No unconverted gamma rays were found, indicating that practically all of the gamma rays are internally converted. More recently Caldwell²⁰ measured three internal conversion electron lines with energies 22.5, 39.0, and 40.8 kev. These he assigned to K, L, and M conversions of a single gamma ray of energy 41.5 ± 0.5 kev.

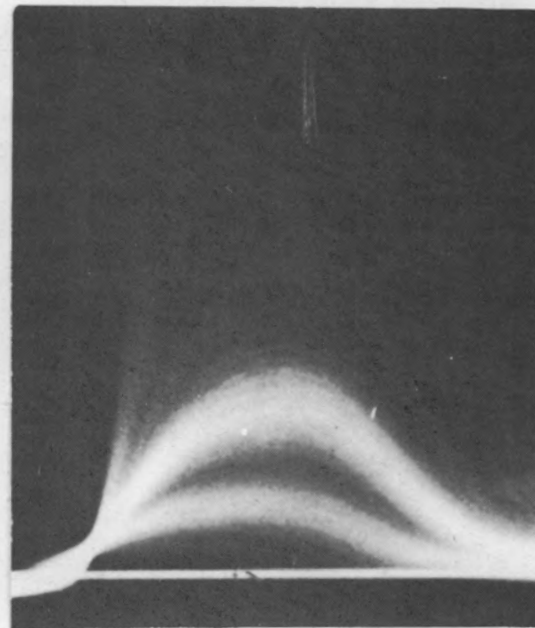
Fig. 13b shows the K x-rays of columbium as detected with a krypton proportional counter. Also shown for comparison are the fluorescent K x-rays from the neighboring elements, zirconium (Fig. 13a) and molybdenum (Fig. 13c). The fluorescent x-rays were excited by the x-rays emitted from Rh^{104} (see below). No evidence of an unconverted gamma ray has been observed. This result confirms that a highly converted isomeric transition occurs in the decay of Cb^{94} .

¹⁹Goldhaber and Muehlhause, loc. cit.

²⁰Caldwell, loc. cit.

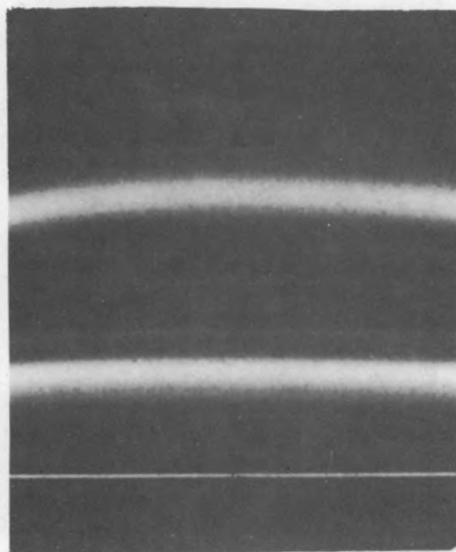


(a)

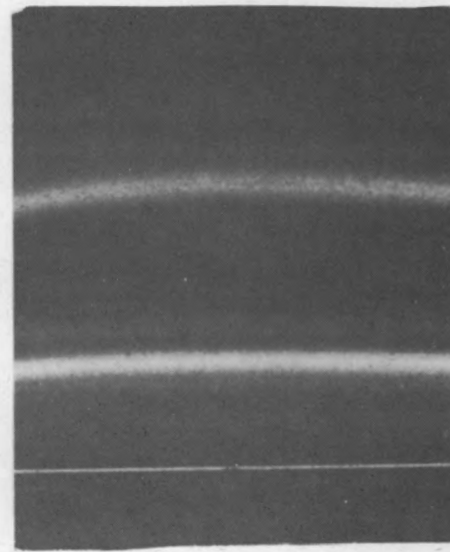


(b)

FIG. 14. Rh^{104} (a) γ RAY AND K X RAY DETECTED WITH THE Xe COUNTER; (b) γ RAY AND K X RAY DETECTED WITH THE NaI COUNTER.

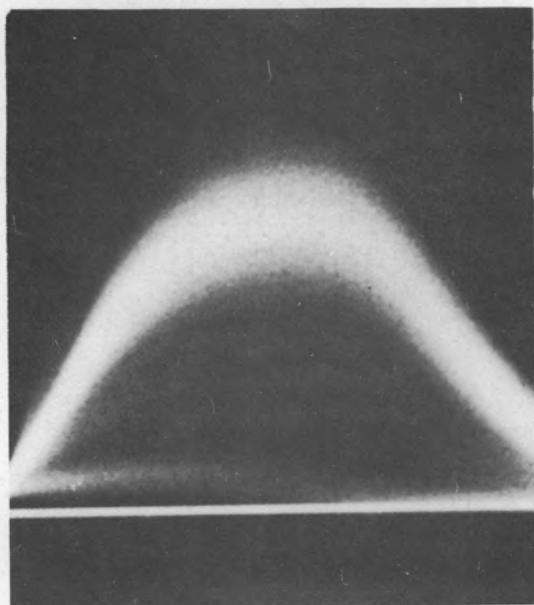


(a)

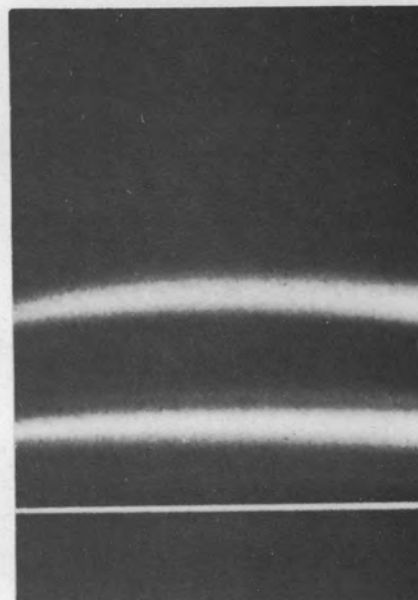


(b)

FIG. 15. RHODIUM K X RAY DETECTED WITH THE Kr COUNTER; (a) RADIOACTIVE SOURCE; (b) FLUORESCENT SOURCE.

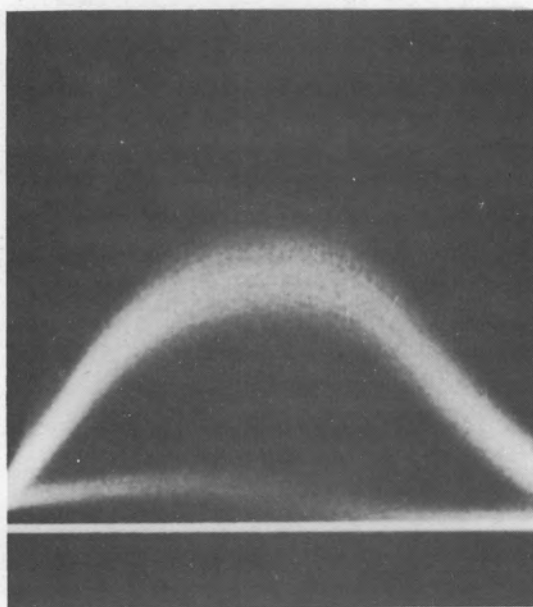


(a)

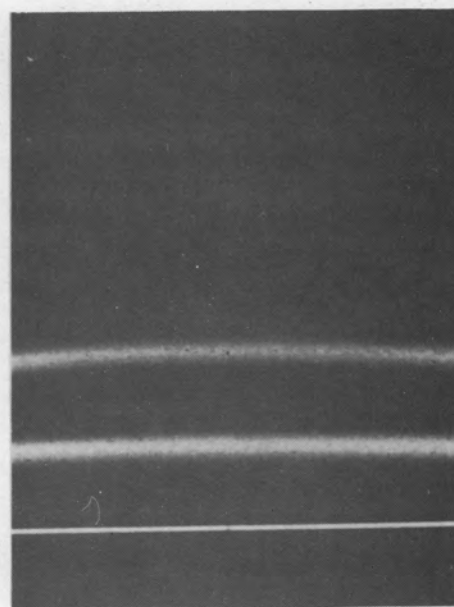


(b)

FIG. 16. Pd¹⁰³ (a) γ RAY AND K X RAY DETECTED WITH THE NaI COUNTER; (b) K X RAY DETECTED WITH THE Kr COUNTER.



(a)



(b)

FIG. 17. In^{113m} (a) γ RAY AND K X RAY DETECTED WITH THE NaI COUNTER; (b) K X RAY DETECTED WITH THE Kr COUNTER.

4.7 Minute Rh¹⁰⁴ Activity

Der Mateosian and Goldhaber²¹ report a 52 keV gamma ray with half-life of 4.7 minutes from rhodium after exposure to slow neutrons in the Brookhaven reactor. Their measurements were made using a NaI scintillation counter.

Fig. 14 shows the gamma and x-radiation from rhodium as detected with a xenon proportional counter and a NaI scintillation counter. The gamma ray shown in Fig. 14a has an energy of 51.5 ± 1.3 keV as determined from comparing its peak height to that of the K x-ray of rhodium.

Fig. 15 compares the x-rays from Rh¹⁰⁴ to the fluorescent x-rays from a rhodium foil excited by the K x-rays from Sb¹²² (see page 59). This result indicates that the transition must be internally converted thus producing rhodium x-rays.

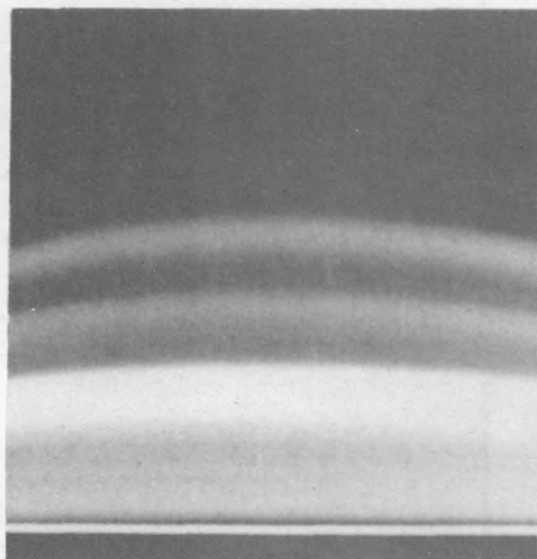
5 Minute Pd Activity

A new short period activity produced by neutron irradiation has been found in palladium. Fig. 16a shows the gamma ray as detected by a NaI counter. This gamma ray has an energy of 173 ± 10 keV which was determined by comparing its pulse height with that of the 279 keV gamma ray from Hg²⁰³.

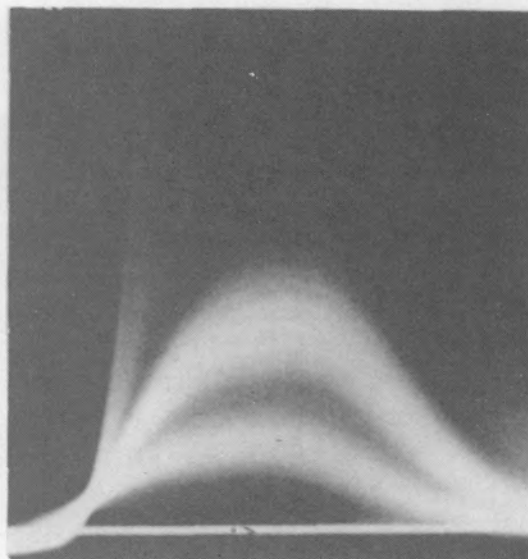
Fig. 16b shows the K x-rays as detected with a krypton counter. Most of the x-rays are emitted following internal conversion of the gamma ray, but some arise from the 13 hour Pd¹⁰⁹ activity which, according to Siegbahn and others,²² decays by beta emission to metastable Ag¹⁰⁹ which

²¹E. der Mateosian and M. Goldhaber, Phys. Rev. 82, 115 (1951).

²²K. Siegbahn, E. Kondiah, and S. Johansson, Nature 164, 405 (1948).

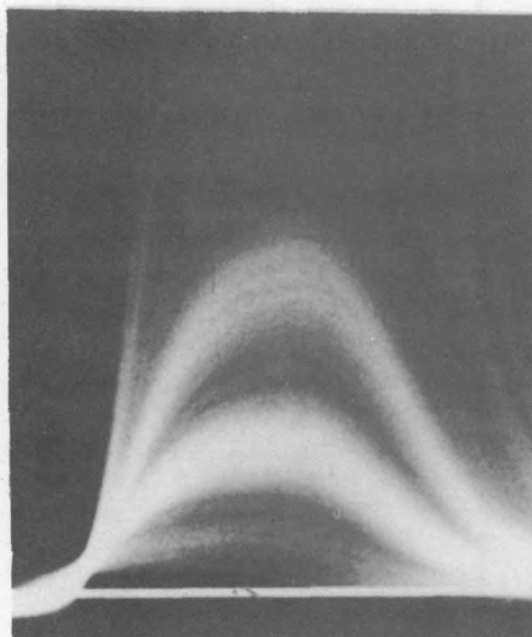


(a)

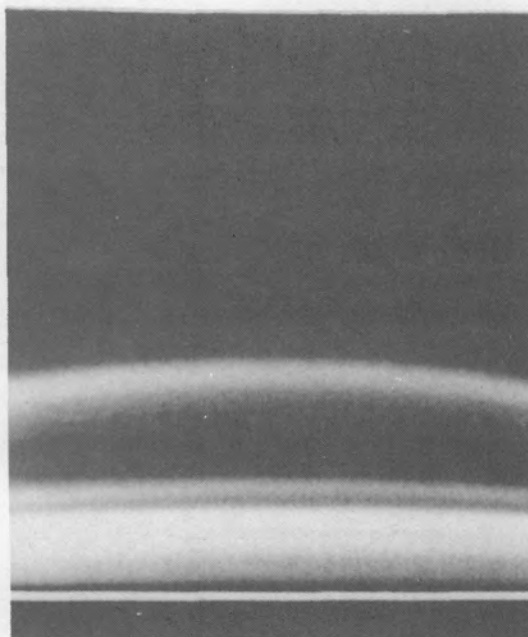


(b)

FIG. 18. Sb^{122} (a) X RAYS AND K X RAY DETECTED WITH THE Xe COUNTER; (b) γ RAYS AND K X RAY DETECTED WITH THE NaI COUNTER.



(a)



(b)

FIG. 19. Dy^{165} (a) γ RAY AND K X RAY DETECTED WITH THE NaI COUNTER; (b) K AND L X RAYS DETECTED WITH THE Xe COUNTER

emits a 87 kev gamma ray that is highly converted thus producing silver x-rays. The disintegration of Pd^{109} and Cd^{109} (discussed earlier) is a case where two different nuclei decaying to the same nucleus (Ag^{109}) have an excited level in common, which in this case is metastable.

2.5 Second In Activity

A new short period activity produced by neutron bombardment has been found in indium. Fig. 17a shows the gamma ray as detected by a NaI counter. This gamma ray has an energy of 153 ± 10 kev as determined from a comparison of its pulse height with that of the 279 kev gamma ray emitted by Hg^{203} .

Fig. 17b shows the K x-rays emitted as detected by a krypton proportional counter. The x-rays indicate that the transition is internally converted.

3.5 Minute Sb^{122} Activity

Der Mateosian and others²³ report a 3.5 minute activity produced in antimony by neutron irradiation. Both internal conversion electrons and characteristic K_{α} radiation of antimony were observed. Aluminum absorption measurements indicated an isomeric transition of 140 kev. This activity was assigned to the (n,γ) reaction with Sb^{121} , as it was not observed in measurements with an isotopically enriched sample of the only other stable antimony isotope (Sb^{123}) upon neutron irradiation.

Fig. 18a shows the gamma radiation, produced by the $(n\gamma)$ reaction

²³E. der Mateosian, M. Goldhaber, C. O. Muehlhause, and M. McKeown, Phys. Rev. 72, 1271 (1947).

with an isotopically enriched Sb^{121} sample, as detected with a xenon proportional counter. Two gamma rays are evident in addition to the antimony K x-rays. The gamma rays have energies of 59 ± 1.5 and 74 ± 2 kev as determined by comparing their pulse heights to that of the K_α x-ray pulse height at 26.4 kev.

Fig. 18b shows the gamma rays as detected by a NaI counter. In this case the resolution is not sufficient to distinguish the two gamma rays, hence only one line at about 65 ± 10 kev is present.

1.25 Minute Dy^{165} Activity

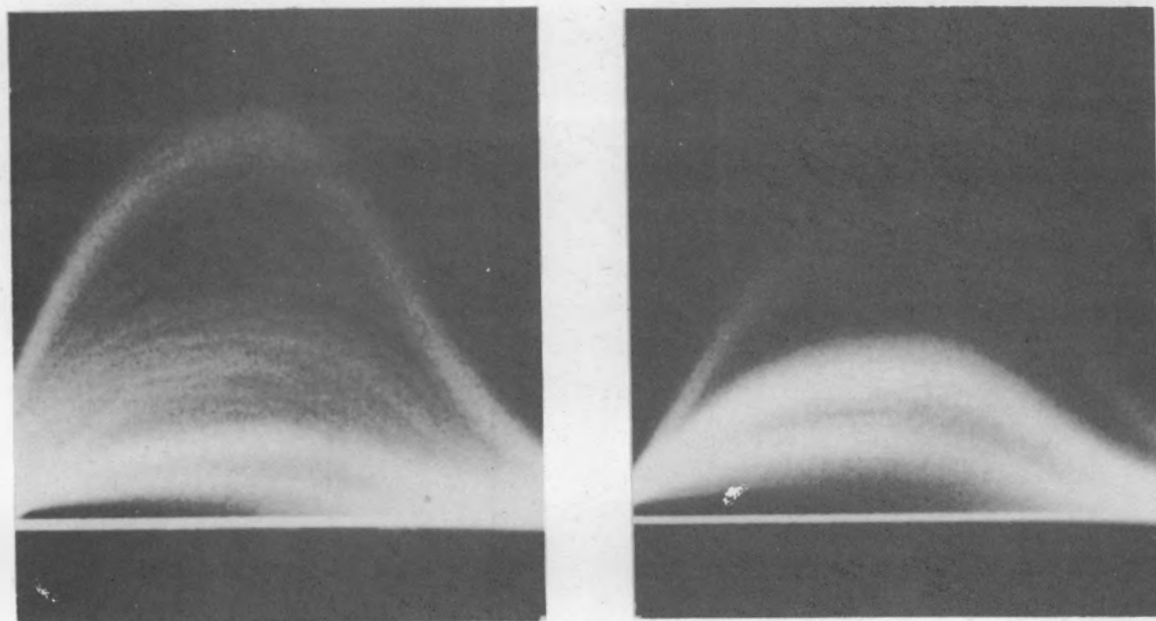
The 1.25 minute K converted gamma activity was initially reported by Flammersfeld.²⁴ Inghram and others²⁵ showed that this activity is isomeric with the 2.6 hour activity and that both of these activities are produced by neutron irradiation of the stable isotope Dy^{164} . Caldwell²⁶, using a permanent magnet beta-ray spectrograph finds five conversion electron lines which he assigned to a single gamma ray of energy 109.0 ± 0.5 kev which converts in the K, L_I , L_{III} , M, and N shells of dysprosium.

Fig. 19a shows the gamma rays and x-rays as detected with a NaI counter. This gamma ray has a value of 102 ± 8 kev as determined by comparing its pulse height to that of the x-ray pulse height at 46 kev.

²⁴A. Flammersfeld, *Zeits. f. Naturforschung*, 1, 190 (1946).

²⁵M. G. Inghram, A. E. Shaw, D. C. Hess, Jr., and R. J. Hayden, *Phys. Rev.* 72, 515 (1947).

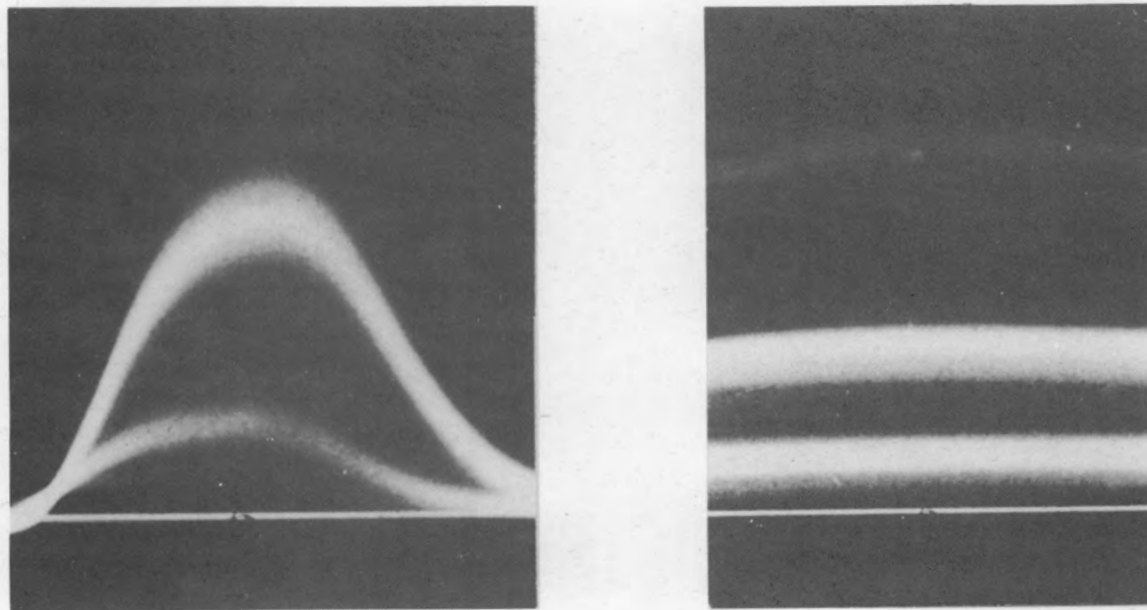
²⁶Caldwell, loc. cit.



(a)

(b)

FIG. 20. Yb^{90} γ RAYS AND K XRAYS DETECTED WITH THE NaI COUNTER (a) 0.5 SEC. ACTIVITY; (b) 6 SEC. ACTIVITY.



(a)

(b)

FIG. 21. Hf^{179} (a) γ RAY AND K XRAY DETECTED WITH THE NaI COUNTER; (b) K AND L XRAYS DETECTED WITH THE Xe COUNTER.

Fig. 19b shows the K and L x-rays from dysprosium as detected by a xenon proportional counter. The gamma ray is too energetic to be detected by the xenon counter.

< 0.5 and 6 Second Yb Activities

Fig. 20a shows an unreported gamma ray of half-life less than 0.5 sec produced in ytterbium by neutron irradiation and detected with a NaI counter. Because of the rapid decay of this gamma ray 8 separate irradiations in the pile and the same number of separate film exposures of 1 sec each were required to produce the photograph shown in Fig. 20a.

This gamma ray has an energy of 455 ± 25 kev as determined by comparing its pulse height with that produced by the 279 kev gamma ray from Hg^{203} .

Fig. 20b shows the gamma rays and x-rays from the 6 second neutron induced activity reported by der Mateosian and Goldhaber²⁷ who observed conversion electrons having energies of about 200 kev as determined by aluminum absorption measurements. The two gamma rays shown in Fig. 20b have energies of 104 ± 8 and 212 ± 15 kev as determined by comparing their pulse heights with that due to the K x-rays at an energy of 53 kev. The 104 kev gamma ray is also shown in Fig. 20a, and is probably due to a dysprosium impurity, but the possibility of a double transition cannot be definitely excluded.

19 Second Hf^{179} Activity

The 19 second hafnium activity was discovered by Flammersfeld²⁸

²⁷E. der Mateosian and M. Goldhaber, Phys. Rev. 76, 187 (1949).

²⁸Flammersfeld, loc. cit.

who observed conversion electrons with energies of about 190 keV produced by slow neutron irradiation of hafnium. Der Mateosian and Goldhaber²⁹ report a neutron induced gamma transition in Hf^{179} with an energy of 215 keV as measured with a NaI scintillation spectrometer.

Fig. 21a shows the gamma ray and x-ray from Hf^{179} as detected with a NaI counter. The gamma ray has an energy of 220 ± 10 keV as determined by comparing its pulse height to that produced by the 279 keV gamma ray from Hg^{203} .

Fig. 21b shows the K and L x-rays from hafnium as detected with a xenon proportional counter. The x-rays are probably associated with an isomeric transition of 161 keV which is believed to be in series with the 220 keV transition. Conversion electrons corresponding to a 161 keV transition have been observed by Burson and his co-workers.³⁰

0.33 Second Ta Activity

The 0.33 second neutron induced activity in tantalum was initially found by Campbell and Good.³¹ Later, Goodrich and Campbell³² reported that the radiation consisted mainly of low energy photons believed to be the L x-rays from tantalum due to a low energy isomeric transition which is highly converted. They concluded that the transition energy E is in the range $E_L < E < E_K$ where E_L and E_K are the binding energies of the L and K shells respectively.

²⁹E. der Mateosian and M. Goldhaber, Phys. Rev. 82, 115 (1951).

³⁰S. B. Burson, K. W. Blair, H. B. Keller and S. Wexler, Phys. Rev. 83, 222 (1951).

³¹E. C. Campbell and W. M. Good, Phys. Rev. 76, 195 (1949).

³²M. Goodrich and E. C. Campbell, Phys. Rev. 79, 418 (1950).

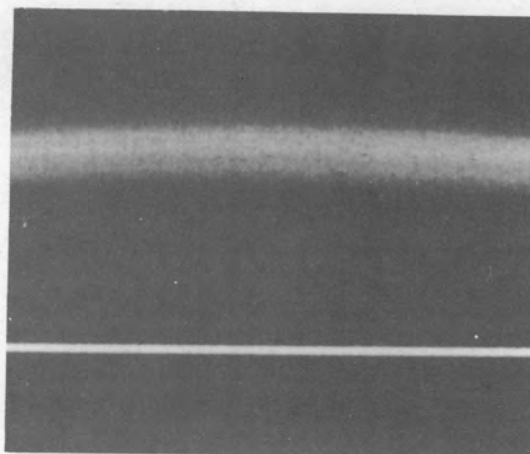
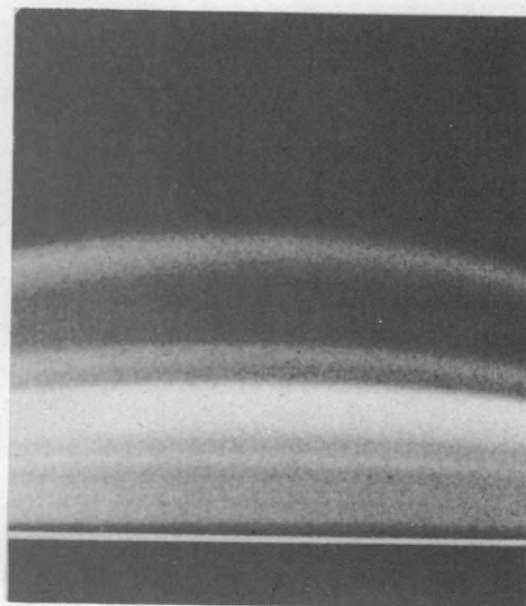


FIG. 22. Ta^{180} L XRAY DETECTED WITH
THE KRYPTON COUNTER.



(a)



(b)

FIG. 23. W^{187} (a) γ RAY AND K XRAY DETECTED
WITH THE NaI COUNTER; (b) K XRAY
DETECTED WITH THE Xe COUNTER.

Fig. 22 shows the L x-rays emitted by tantalum as detected by a krypton counter. Fifteen separate irradiations in the pile for a period of one second each and fifteen subsequent film exposures of one second each were required in making the photograph shown in Fig. 22. Comparison of these x-rays with those emitted by long life Hf^{181} confirmed that the x-rays in Fig. 22 are from tantalum.

5.5 Second W Activity

Der Mateosian and Goldhaber³³ report finding conversion electrons of 80 kev energy and half-life of 5.5 seconds produced by slow neutron irradiation of tungsten. Their energy measurements were obtained by aluminum absorption.

Fig. 23 shows the x-rays from tungsten as detected by a NaI crystal and a xenon proportional counter. In Fig. 23a there is evidence of a weak gamma ray with energy slightly greater than the K x-ray lines (58-69 kev). This additional evidence is in accordance with Mateosian and Goldhaber's findings.

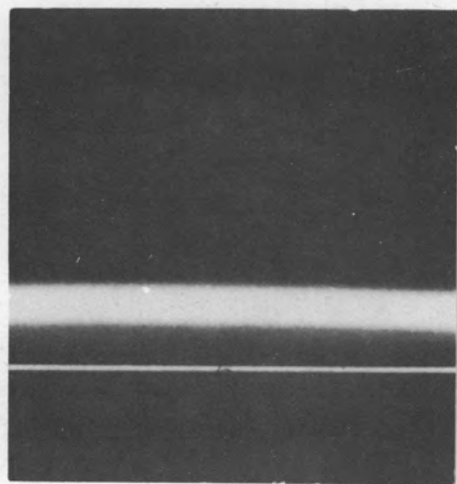
1.5 Minute Ir^{192} Activity

The 1.5 minute neutron induced activity in iridium was reported first by McMillan, Kamen and Ruben.³⁴ Goldhaber and others³⁵ later reported two gamma rays with energies of approximately 60 kev and 30 kev,

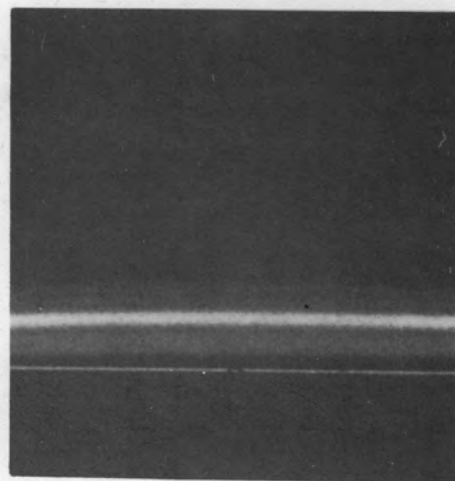
³³E. der Mateosian and M. Goldhaber, Phys. Rev. 76, 187 (1949).

³⁴E. McMillan, M. Kamen and S. Ruben, Phys. Rev. 52, 375 (1937).

³⁵M. Goldhaber, C. O. Muehlhause and S. H. Turkel, Phys. Rev. 71, 372 (1947).



(a)



(b)

FIG. 24. Ir^{192} (a) L XRAY DETECTED WITH THE Xe COUNTER; (b) L XRAY DETECTED WITH THE Xe COUNTER WITH COPPER ABSORBER.

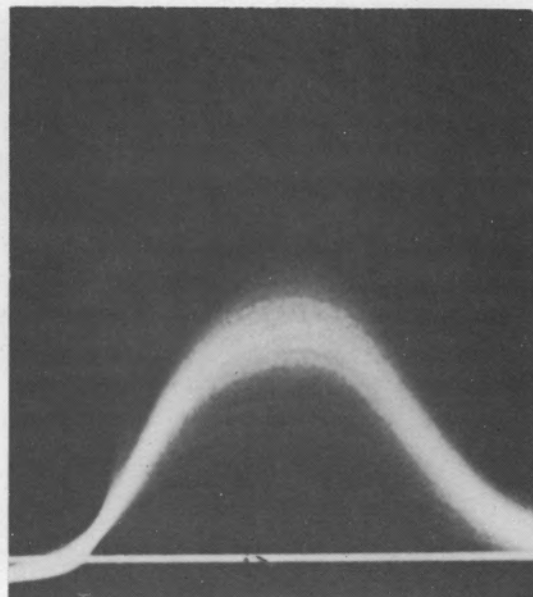
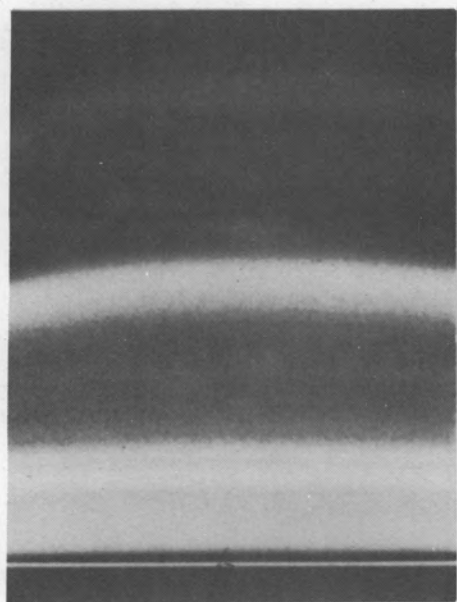


FIG. 25. U^{239} (a) γ RAY AND L XRAY DETECTED WITH THE Xe COUNTER; (b) γ RAY DETECTED WITH THE NaI COUNTER.

as well as strong L x-rays of iridium. They were unable, however, by critical absorption to show that there is a unique gamma ray in the region of about 30 kev. Caldwell³⁶ finds four conversion electron lines which were assigned to a single gamma ray with energy of 57.4 ± 0.5 kev which converts in the L_I, L_{III}, M, and N shells of iridium. He was also unable to obtain evidence indicating a discrete lower energy gamma ray.

Fig. 24 shows the L x-rays of iridium as detected by a xenon proportional counter. There is no evidence of an unconverted gamma ray of intensity near that of the x-ray. These x-rays are presumed to follow the internal conversion process. Fig. 24b was given roughly 10 times the exposure of Fig. 24a, with a thin copper foil inserted between the source and the detector to absorb the L x-rays of iridium, in an attempt to observe any unconverted gamma rays. The copper foil strongly attenuates the L x-rays of iridium, but it would have little effect on a gamma ray with an energy of the order of 25 kev. The fact that no radiation more energetic than the L x-rays is observed indicates that the transition is highly converted.

23.5 Minute U²³⁹ Activity

Meitner and others³⁷ first reported a uranium isotope produced by neutron capture with the half-life 23 minutes. Feather and Krishnan³⁸ from absorption measurements report the disintegration of U²³⁹ involves

³⁶Caldwell, loc. cit.

³⁷L. Meitner, O. Hahn and F. Strassman, *Zeits f Physik*, 106, 249 (1937).

³⁸N. Feather and R. S. Krishnan, *Proc. Camb. Phil. Soc.* 43, 267 (1947).

beta rays having an upper energy limit of 1.20 ± 0.02 Mev and a gamma ray with energy of 76 ± 3 kev. They also found evidence for electrons of less energy (about 0.1 per disintegration) and more penetrating gamma rays of relatively low intensity. Quantum radiations corresponding roughly to the L x-rays, to be expected following the internal conversion of the low energy gamma ray, were also detected. Slätis³⁹ reports two internal conversion lines plus a continuous beta ray spectra from investigation with a magnetic lens spectrograph of the radiation from U^{239} . The two conversion lines are produced by the L and M conversion of a 73 kev nuclear gamma ray which is emitted by an excited neptunium nucleus following beta decay in the uranium. This beta ray has a maximum energy of 1.12 Mev and occurs in 97 per cent of the disintegrations. There is another beta ray with maximum energy of 2.06 Mev which decays directly to the ground state of neptunium in the remaining 3 per cent of the disintegrations.

Fig. 25 shows the gamma ray from U^{239} as detected by a NaI crystal and xenon proportional counter. This gamma ray has an energy of 74 ± 2 kev as determined from its pulse height in the xenon counter photograph compared to the distance to the lower energy line produced by the escape from the counter of a xenon K x-ray (29.7 kev). The xenon counter also detects the L x-rays from neptunium which are emitted subsequent to internal conversion in the L shell. The gamma transition is not energetic enough to produce conversion in the K shell, and therefore no K x-rays are in evidence.

³⁹H. Slätis, Arkiv Mat. Astron. Fysik 35A, No. 3 (1948).

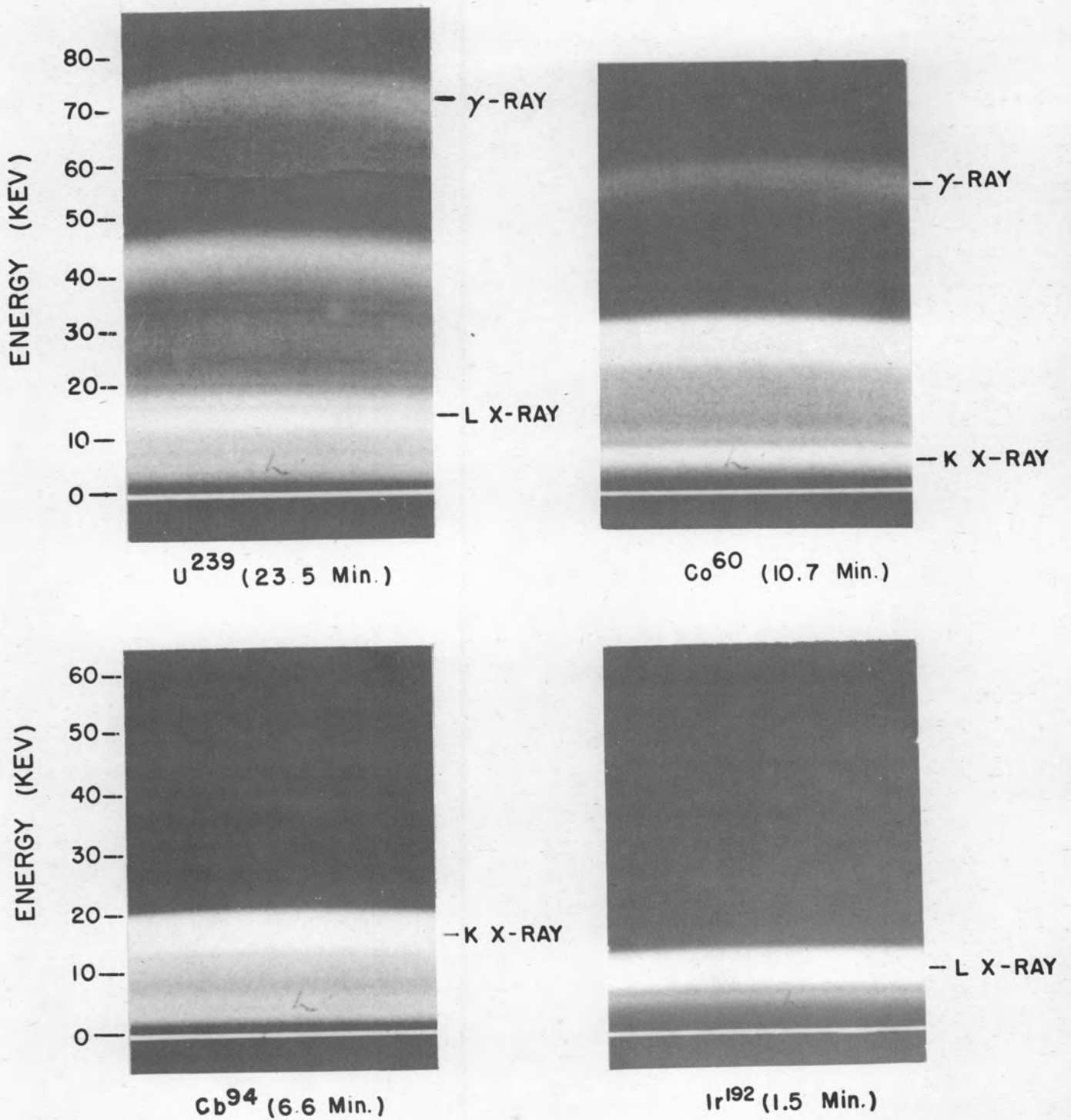


FIG. 26
GAMMA AND X-RADIATION FROM VARIOUS
RADIOACTIVE NUCLEI AS DETECTED BY A
XENON-METHANE PROPORTIONAL COUNTER

CHAPTER IV

ANALYSIS OF DATA

Partial Internal Conversion Coefficients

The emission of a K or L conversion electron from a radioactive atom will leave the atom ionized in the K or L electron shell, and consequently when this shell fills, an x-ray of the K or L series can be emitted. The detection of these x-rays should give a quantitative measurement of how many K or L conversion electrons have been emitted provided that the fluorescent yield of the decaying atom is taken into account.

A time exposure photograph of the output pulses from a proportional counter as displayed on the screen of an oscilloscope indicates the relative number of x-rays and gamma rays emitted by a radioactive sample. Such photographs are shown in Fig. 26. Scanning the film with a recording microphotometer gives a permanent record of the relative number of counts per unit energy range from which the partial conversion coefficient may be calculated as follows.

$$R = \left(\frac{N_{K,L}}{N_\gamma} \right) \text{ WTE} \quad (18)$$

$$\therefore \alpha_{K,L} = \frac{N_{K,L}}{N_\gamma} = \frac{R}{\text{WTE}} \quad (19)$$

where R = ratio of x-ray intensity of a given shell to gamma ray intensity as determined by comparing areas under the appropriate pulse peaks of the microphotometer tracing.

TABLE III
PARTIAL INTERNAL CONVERSION COEFFICIENTS

Element	Half-Life (Minutes)	Gamma Ray Energy (kev)	R Relative Intensity of X-Ray to γ -Ray	W Fluorescent Yield	T Relative Transmission of Beryllium Absorber	E Relative Efficiency of Xenon Proportional Counter	ALPHA Partial Internal Conversion Coefficient	
							K Shell α_K	L Shell α_L
$^{60}_{27}\text{Co}$	10.7	59.0	0.26	0.32	0.005*	4.69	35.0	
$^{94}_{41}\text{Cb}$	6.6	41.5	>110	0.67	0.90	1.61	>100	
$^{192}_{77}\text{Ir}$	1.4	57.4	>80	~0.50	0.09*	4.52		>400
$^{239}_{92}\text{U}$	23.5	74.0	0.85	0.67	0.90	7.29		0.20

$$\alpha = \frac{R}{W T E}$$

*Includes correction for absorption due to counter walls

W = fluorescent yield of the given electron shell.¹

T = relative transmission efficiency of the beryllium absorber
(used to stop any beta rays or conversion electrons) for the
given x-ray to the gamma ray.²

E = relative efficiency of the xenon proportional counter for the
x-ray compared to the gamma ray (see Fig. 9).

The results obtained for various radioactive nuclei are shown in Table III. These results will be in error if the decay schemes now believed correct for the given isotopes should later prove to be more complex. For instance, if K or L capture occurs in any of the nuclei listed in Table III, this would produce x-rays other than those resulting from internal conversion and the measured conversion coefficient would be too large. Also, if there is a second gamma ray that is almost wholly converted and is therefore unobservable, there would be additional x-rays which would not belong to the transition being studied.

The value of α_L listed in Table II for U^{239} is higher than that found by Slätis³ (0.14). This is probably due in part to the absorption within the uranium sample of the unconverted gamma ray. Assuming a sample thickness of 25 mg/cm^2 and using a mass absorption coefficient⁴ of $4 \text{ cm}^2/\text{gm}$ for the 73 keV gamma ray indicates that approximately $4 \times 0.025 \times 0.5$ or 5 per cent of the gamma rays are absorbed (where the

¹R. M. Steffen, O. Huber and F. Humbel, *Helv. Phys. Acta* 22, 167 (1949).

²Compton and Allison, *op. cit.*, p. 800.

³H. Slätis, *Arkiv. Mat. Astron. Fysik* 35A, No. 3 (1948).

⁴Compton and Allison, *loc. cit.*

average path length for the gamma rays was taken to be one-half the sample thickness). If all these produce photoelectrons from the L shell, then the measured value of α_L will be too large by this absorbed fraction. A corrected value of 0.15 is thus obtained for α_L . In the case of Co^{60} a correction of this magnitude is negligible relative to the value obtained for α_K .

In the case of Ir^{192} and U^{239} the gamma transition is not energetic enough to produce K conversion, therefore L conversion is the predominant type.

Conclusion

The occurrence of nuclear isomerism among nuclei of odd mass number can be explained in a qualitative way by the nuclear shell model.⁵ The model of Mayer is based on the succession of energy levels of a single particle in a potential between that of a three dimensional harmonic oscillator and a square well. The order of the energy levels in this model, if spin-orbit coupling is assumed, is as follows:

$(1s_{1/2})^2$	2
$(2p_{3/2})^4 (2p_{1/2})^2$	8
$(3d_{5/2})^6 (3d_{3/2})^4 (2s_{1/2})^2$	20
$(4f_{7/2})^8 (4f_{5/2})^6 (3p_{3/2})^4 (3p_{1/2})^2 (5g_{9/2})^{10}$	50

⁵M. Goeppert-Mayer, Phys. Rev. 78, 16 (1950); and E. Feenberg and K. C. Hammack, Phys. Rev. 75, 1877 (1949).

$$(5g_{7/2})^8 (4d_{5/2})^6 (4d_{3/2})^4 (3s_{1/2})^2 (6h_{11/2})^{12} \quad 82$$

$$(6h_{9/2})^{10} (5f_{7/2})^8 (5f_{5/2})^6 (4p_{3/2})^4 (4p_{1/2})^2 (7i_{13/2})^{14} \quad 126$$

where each horizontal line describes a shell and the total number of like nucleons required to fill all the preceding shells is given at the end of each line. An even number of identical nucleons in any orbit with total angular momentum quantum number j will always couple to give a spin zero, and an odd number of identical nucleons in a state j will couple to give a total spin j .

The stability of nuclei containing 2, 8, 20, 28, 50, 82 or 126 neutrons or protons⁶ is explained by the existence of closed shells in these nuclei. Near the end of a shell, where isomers frequently occur, are states with quite different spins whose energies are not too far apart. The competition between these adjacent states may result in a nucleon going into the next higher shell rather than filling up the lower, incomplete shell. Wherever the shell theory predicts two closely spaced levels differing by three or four units in spin, isomerism becomes a likely possibility.

All of the isomers with odd mass numbers⁷ listed in Table IV can be correlated with the shell model. Se^{77} ($N = 43$) and Ag^{109} ($Z = 47$) can

⁶W. M. Elsassner, *J. de phys. et rad.* **2**, 635 (1934); and M. Goeppert-Mayer, *Phys. Rev.* **74**, 235 (1948).

⁷"Nuclear Data", circular 499, National Bureau Standards, Washington, D. C. (1950).

TABLE IV
SUMMARY OF EXPERIMENTAL DATA

Isomer	Transition Energy (kev)	Half-life	α_{total}^*	τ_{γ} (sec)	Remarks
$^{27}\text{Co}^{60}$	58.5	10.7 min	~ 40	2.6×10^4	See Fig. 26
$^{34}\text{Se}^{77}$	130	17.5 sec	(0.9)	3.3×10	
$^{41}\text{Cb}^{94}$	41.5	6.6 min	~ 500	2.0×10^5	See Fig. 26
$^{45}\text{Rh}^{104}$	51.5	4.7 min	~ 25	7.3×10^3	See Fig. 14
$^{46}\text{Pd}^?$	173	5 min	~ 1	6.0×10^2	See Fig. 16
$^{47}\text{Ag}^{109}$	87	39 sec	(24)	9.7×10^2	
$^{49}\text{In}^?$	153	2.5 sec	~ 1	5.0	See Fig. 17
$^{51}\text{Sb}^{122}$	59,74	3.5 min	$\sim 25^{**}$	5.5×10^3	See Fig. 18
$^{66}\text{Dy}^{165}$	102	1.3 min	(50)	4.0×10^3	
^{70}Yb	455	< 0.5 sec	(0.06)	3.0×10^{-1}	
^{70}Yb	212	6 sec	(~ 1.2)	1.3×10	
$^{72}\text{Hf}^{179}$	161	19 sec	(~ 32)	6.3×10^2	
$^{74}\text{W}^{183}$	~ 80	5.5 sec	(130)	7.2×10^2	
$^{77}\text{Ir}^{192}$	57.4	1.5 min	~ 500	4.5×10^4	See Fig. 26

*The conversion coefficients listed in parentheses are given by Goldhaber and Sunyar⁹ by adding an estimated correction for L conversion to the calculated K-shell coefficients⁹ (page 13).

**Conversion arbitrarily assigned to 59 kev transition.

both have the competing orbits $2p_{1/2}$ and $1g_{9/2}$ which would account for their isomeric transitions. For Dy^{165} ($N = 99$) the transition is possibly due to the competition between the $6h_{9/2}$ and $4p_{1/2}$ orbits. The isomeric transitions arising from Hf^{179} ($N = 107$) and W^{183} ($N = 109$) may be explained by competition between the $6h_{11/2}$ and $4p_{3/2}$ states.

For the isomers with A even listed in Table IV, it will be noted that all have N odd and Z odd. This is in accordance with Mattauch's⁸ observation that there are no isomeric pairs with N even and Z even. More recently published data indicate exceptions (Hf^{180} and Pb^{204}) to this "rule".

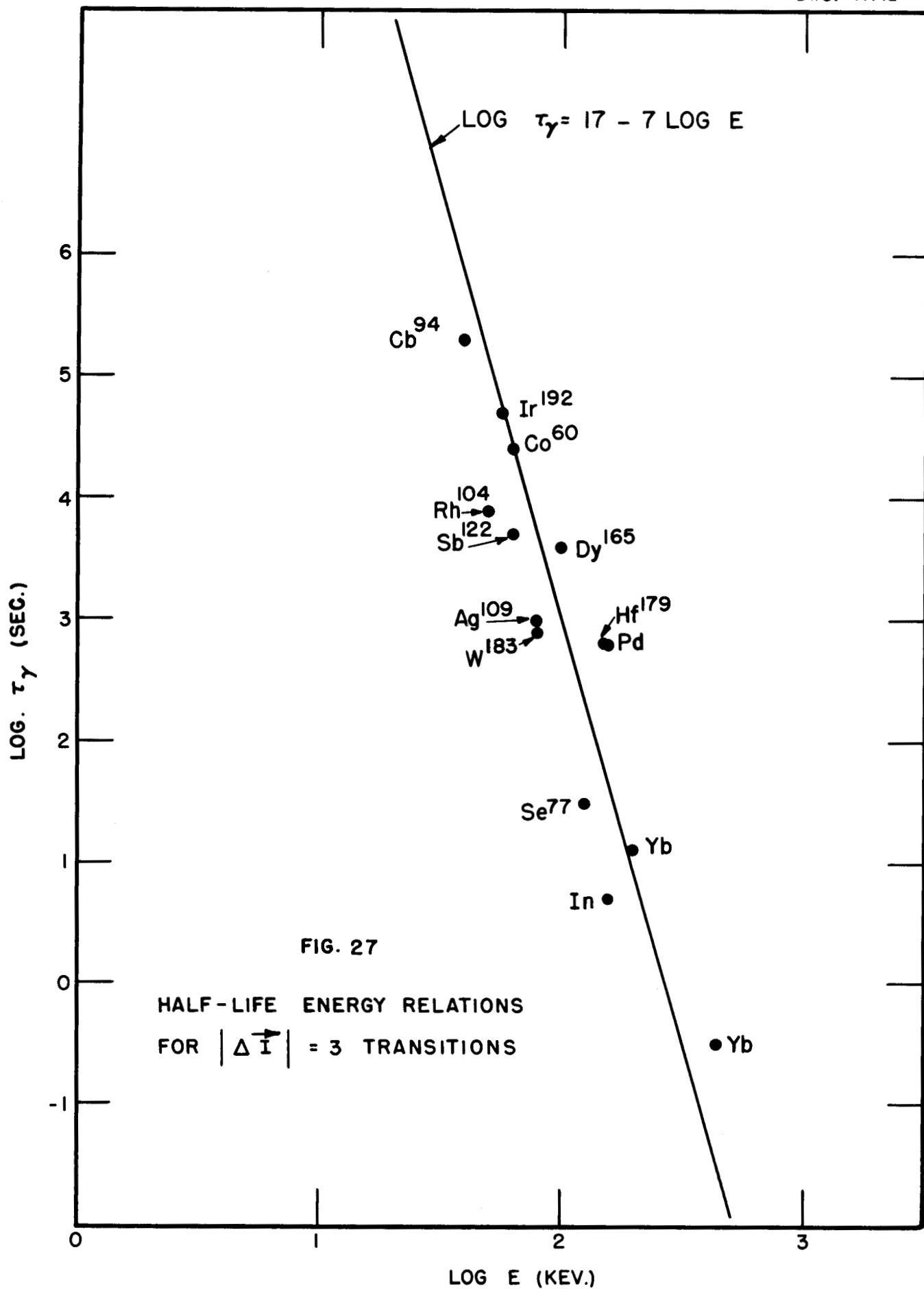
In Fig. 27, $\log \tau_\gamma$ (sec) is plotted versus $\log E$ (kev), where $\tau_\gamma = \tau_{\text{exp}} (1 + \alpha)$, for the isomers listed in Table IV. According to Goldhaber and Sunyar⁹ these isomers belong to the group characterized by $|\Delta \vec{I}| = 3$. They obtain the following empirical formula for transitions within this group.

$$\log \tau_\gamma \text{ (sec)} = 17.3 - 7 \log E(\text{kev}) \quad (20)$$

An inspection of Fig. 27 indicates that a little better representation of the data is obtained by changing the constant term in the above equation to 17.0. This formula is identical to that calculated by Weisskopf for magnetic radiation of multipole order 3 (see equation 5) where R is given the value 7.7×10^{-13} cm (i.e. $A = 135$).

⁸J. Mattauch, *Zeits. f. Physik* 117, 246 (1941).

⁹M. Goldhaber and A. W. Sunyar, *Quarterly Progress Report*, BNL 103, 3 (1951).



Summary

1. A short period neutron induced gamma activity was discovered in Pd ($E = 173$ kev, $\tau = 5$ min), In ($E = 153$ kev, $\tau = 2.5$ sec) and Yb ($E = 455$ kev, $\tau < 0.5$ sec).
2. Two gamma rays ($E = 59$ and 74 kev) were found to be associated with the 3.5 minute Sb^{122} activity which was previously reported to emit only a single gamma ray.
3. The fluorescent yield for the K shell of krypton (0.70) and xenon (0.85) was measured.
4. The efficiency of a xenon-methane filled proportional counter as a function of energy of the incident electromagnetic radiation was measured.
5. Partial internal conversion coefficients were measured for Co^{60} ($\alpha_K = 35$), Cb^{94} ($\alpha_K > 100$), Ir^{192} ($\alpha_L > 400$) and U^{239} ($\alpha_L = 0.2$).

BIBLIOGRAPHY

- Agno, M. *Nuovo Cimento* 1, 33 (1943).
- Amaldi, E., D'Agostino, O., Fermi, E., Pontecorvo, B., Rosetti, F., and Segré, E. *Proceedings of the Royal Society* A149, 522 (1935).
- Arnold, J. R., and Sugarman, N. *Journal of Chemical Physics* 15, 703 (1947).
- Auger, P. *Annales de Physique* 6, 183 (1926).
- Bell, P. R. *Science* 112, 7 (1950).
- Bernstein, W., Brewer, H. G., Jr., and Rubinson, W. *Nucleonics* 6, No. 2, 39 (1950).
- Bradt, H., Gugelot, P. C., Huber, O., Medicus, H., Preiswerk, P., Scherrer, P., and Steffer, R. *Helvetica Physica Acta* 20, 153 (1947).
- Burson, S. B., Blair, K. W., Keller, H. B., and Wexler, S. *Physical Review* 83, 222 (1951).
- Caldwell, R. L. *Physical Review* 78, 407 (1950).
- Campbell, E. C., and Good, W. M. *Physical Review* 76, 195 (1949).
- _____, and Goodrich, M. *Physical Review* 78, 640 (1950).
- Compton, A. H., and Allison, S. K. X-rays in Theory and Experiment (New York: D. Van Nostrand Co., Inc., 1935).
- der Mateosian, E., and Goldhaber, M. *Physical Review* 76, 187 (1949).
- _____, and Goldhaber, M. *Physical Review* 82, 115 (1951).
- _____, Goldhaber, M., Muehlhause, C. O., and McKeown, M. *Physical Review* 72, 1271 (1947).
- Deutsch, M., Elliott, L. G., and Roberts, A. *Physical Review* 68, 193 (1945).
- Ellis, C. D. *Proceedings of the Royal Society* A99, 261 (1921).
- Elsasser, W. M. *Journal de Physique et le Radium* 5, 635 (1934).
- Fairstein, E. A Sweep Type Differential and Integral Discriminator, ORNL 893, Series A (1951).

- Feather, N., and Krishnan, R. S. Proceedings of the Cambridge Philosophical Society 43, 267 (1947).
- Feenberg, E., and Hammack, K. C. Physical Review 75, 1877 (1949).
- Fermi, E., Amaldi, E., D'Agostino, O., Rosetti, F., and Segré, E. Proceedings of the Royal Society, A146, 483 (1934).
- Flammersfeld, A. Zeitschrift Für Naturforschung 1, 190 (1946).
- Gellman, H., Griffith, B. A., and Stanley, J. P. Physical Review 80, 866 (1950).
- Glendenin, L. E. Nucleonics 2, No. 1, 12 (1948).
- Goeppert-Mayer, M. Physical Review 74, 235 (1948).
- _____, Physical Review 78, 16 (1950).
- Goertzel, G., and Lowen, I. S. Physical Review 67, 203 (1945).
- Goldhaber, M., and Muehlhause, C. O. Physical Review 74, 1248 (1948).
- _____, Muehlhause, C. O., and Turkel, S. H. Physical Review 71, 372 (1947).
- _____, and Sunyar, A. W. Quarterly Progress Report, BNL 103 (S-9), 3 (1951).
- Goodrich, M., and Campbell, E. C. Physical Review 79, 418 (1950).
- Hill, J. M., and Sheperd, L. R. Proceedings of the Physical Society A63, 126 (1950).
- Inghram, M. G., Shaw, A. E., Hess, D. C., Jr., and Hayden, R. J. Physical Review 72, 515 (1947).
- Insch, G. M. Philosophical Magazine 41, 857 (1950).
- Jordan, W. H., and Bell, P. R. Reviews of Scientific Instruments, 18, 703 (1947).
- Korff, S. A., and Present, R. D. Physical Review 65, 274 (1944).
- Lind, D. A., Brown, J. R., and DuMond, J. W. Physical Review 76, 1838 (1949).
- Mattauch, J. Zeitschrift Für Physik 117, 246 (1941).
- McMillan, E., Kamen, M., and Ruben, S. Physical Review 52, 375 (1937).

- Meitner, L., Hahn, O., and Strassman, F. Zeitschrift Für Physik 106, 249 (1937).
- Montgomery, C. G., and Montgomery, D. D. Physical Review 57, 1030 (1940).
- Morton, G. A., and Mitchell, J. A. Nucleonics 4, 16 (1949).
- "Nuclear Data", circular 499, National Bureau of Standards, Washington, D. C. (1950).
- Rose, M. E., Goertzel, G. H., Spinrad, B. I., Harr, J., and Strong, P. Physical Review 83, 79 (1951).
- _____, and Korff, S. Physical Review 59, 850 (1941).
- Siegbahn, K., Kondaiah, E., and Johansson, S. Nature 164, 405 (1949).
- Slätis, H. Arkiv for Matematik, Astronomi och Fysik 35A, No. 3 (1948).
- Steffen, R. M., Huber, O., and Humbel, F. Helvetica Physica Acta 22, 167 (1949).
- Taylor, H. M., and Mott, N. F. Proceedings of the Royal Society A138, 665 (1932).
- _____, and Mott, N. F. Proceedings of the Royal Society A142, 215 (1933).
- von Weizsäcker, C. F. Naturwissenschaften 24, 813 (1936).
- West, D., and Rothwell, P. Philosophical Magazine 41, 873 (1950).